ANALYSIS OF CAPSULE T FROM THE H. B. ROBINSON UNIT 2 REACTOR VESSEL RADIATION SURVEILLANCE PROGRAM (WCAP-10304)

EPRI RESEARCH PROJECT 1021-3
TOPICAL REPORT

March 1983

Prepared by

WESTINGHOUSE ELECTRIC CORPORATION
Nuclear Technology Division
P. O. Box 355
Pittsburgh, Pennsylvania 15230

T. R. Mager, Principal Investigator

Prepared for

ELECTRIC POWER RESEARCH INSTITUTE
3412 Hillview Avenue
Palo Alto, California 94304

T. U. Marston, Project Manager

ANALYSIS OF CAPSULE T FROM THE H. B. ROBINSON UNIT 2 REACTOR VESSEL RADIATION SURVEILLANCE PROGRAM (WCAP-10304)

EPRI RESEARCH PROJECT 1021-3 TOPICAL REPORT

S. E. Yanichko
S. L. Anderson
R. P. Shogan
R. G. Lott

March 1983

Prepared by

WESTINGHOUSE ELECTRIC CORPORATION
Nuclear Technology Division
P. O. Box 355
Pittsburgh, Pennsylvania 15230

T. R. Mager, Principal Investigator

Prepared for

ELECTRIC POWER RESEARCH INSTITUTE
3412 Hillview Avenue
Palo Alto, California 94304

T. U. Marston, Project Manager

LEGAL NOTICE

This report was prepared by Westinghouse Electric Corporation (WESTINGHOUSE) as an account of work sponsored by the Electric Power Research Institute, Inc. (EPRI). Neither EPRI, members of EPRI, nor WESTINGHOUSE, nor any person acting on behalf of either:

a. Makes any warranty or representation, express or implied, with respect to the accuracy, completeness, or usefulness of the information contained in this report, or that the use of any information, apparatus, method, or process disclosed in this report may not infringe privately owned rights; or

b. Assumes any liabilities with respect to the use of, or for damages resulting from the use of, any information, apparatus, method, or process disclosed in this report.

TABLE OF CONTENTS

LIST OF ILLUSTRATIONS

LIST OF ILLUSTRATIONS (cont)

LIST OF TABLES

LIST OF TABLES (cont)

SECTION 1
SUMMARY OF RESULTS

The analysis of the reactor vessel material contained in Capsule T, the third reactor vessel material surveillance capsule which was removed from the Carolina Power and Light Company H. B. Robinson Unit 2 reactor pressure vessel after approximately 7.2 effective full power years of operation, led to the following conclusions:

- The surveillance capsule received an average fast neutron fluence ($E > 1$ MeV) of 4.11×10^{19} n/cm^2 compared to a calculated fluence of 3.81×10^{19} n/cm^2.

- Irradiation of base metal plate material to 4.11×10^{19} n/cm^2 resulted in a 42°C increase in the 41-joule transition temperature when compared with unirradiated values. The transition temperature increase, when compared with prior results after irradiation to 3.69×10^{18} n/cm^2, indicates that the increased neutron fluence produced an additional 34°C increase in transition temperature.

- Submerged arc weld metal irradiated to 4.11×10^{19} n/cm^2 showed a 41-joule transition temperature increase of 158°C compared to a 97°C increase for prior tests irradiated at 5.84×10^{19} n/cm^2.

- Comparisons of the 41-joule transition temperature increases for the H. B. Robinson Unit 2 surveillance materials with Regulatory Guide 1.99 Revision 1 predictions show that the increases after irradiation to 4.11×10^{19} n/cm^2 are significantly less than predicted.

SECTION 2
INTRODUCTION

This report presents the results of the examination of Capsule T, the third capsule to be removed from the reactor in the continuing surveillance program which monitors the effects of neutron irradiation on the H. B. Robinson Unit 2 reactor pressure vessel materials under operating conditions.

The surveillance program for the reactor pressure vessel materials was designed and recommended by the Westinghouse Electric Corporation. A description of the surveillance program and the preirradiation mechanical properties of the reactor vessel materials are presented in WCAP-7373 [1]. The surveillance program was planned to cover the 40-year life of the reactor pressure vessel and was based on ASTM E185-66. Westinghouse Nuclear Technology Division personnel were contracted for the preparation of procedures for removing the capsule from the reactor and its shipment to the Westinghouse Research and Development Laboratory, where the postirradiation mechanical testing of the Charpy V-notch impact and tensile surveillance specimens was performed.

This report summarizes testing and the postirradiation data obtained from the third surveillance capsule (Capsule T) removed from the H. B. Robinson Unit 2 reactor vessel and discusses the analysis of these data. The data are also compared to results obtained from the two previous surveillance capsules (Capsules S and V)[2,3,4] which were tested as part of the program.

SECTION 3
BACKGROUND

The ability of the large steel pressure vessel containing the reactor core and its primary coolant to resist fracture constitutes an important factor in ensuring safety in the nuclear industry. The beltline region of the reactor pressure vessel is the most critical region of the vessel because it is subjected to significant fast neutron bombardment. The overall effects of fast neutron irradiation on the mechanical properties of low alloy ferritic pressure vessel steels such as SA302 Grade A (base material of the H. B. Robinson Unit 2 reactor pressure vessel beltline) are well documented in the literature. Generally, low alloy ferritic materials show an increase in hardness and tensile properties and a decrease in ductility and toughness under certain conditions of irradiation.

A method of performing analyses to guard against fast fracture in reactor pressure vessels has been presented in "Protection Against Non-ductile Failure," Appendix G to Section III of the ASME Boiler and Pressure Vessel Code. The method utilizes fracture mechanics concepts and is based on the reference nil-ductility temperature RT_{NDT}.

RT_{NDT} is defined as the greater of either the drop weight nil-ductility transition temperature (NDTT per ASTM E-208) or the temperature 60°F less than the 50 ft lb (or 35-mil lateral expansion) temperature as determined from Charpy specimens oriented normal to the major working direction of the material. The RT_{NDT} of a given material is used to index that material to a reference stress intensity factor curve (K_{IR} curve) which appears in Appendix G of the ASME Code. The K_{IR} curve is a lower bound of dynamic, crack arrest, and static fracture toughness results obtained from several heats of pressure vessel steel. When a given material is indexed to the K_{IR} curve, allowable stress intensity factors can be obtained for this material as a function of temperature. Allowable operating limits can then be determined utilizing these allowable stress intensity factors.

RT_{NDT} and, in turn, the operating limits of nuclear power plants can be adjusted to account for the effects of radiation on the reactor vessel material properties. The radiation embrittlement or changes in mechanical properties of a given reactor pressure vessel steel can be monitored by a reactor surveillance program such as the H. B. Robinson Unit 2 Reactor Vessel Radiation Surveillance Program,[1] in which a surveillance capsule is periodically removed from the operating nuclear reactor and the encapsulated specimens are tested. The increase in the Charpy V-notch 30 ft lb temperature (ΔRT_{NDT}) due to irradiation is added to the original RT_{NDT} to adjust the RT_{NDT} for

radiation embrittlement. This adjusted RT_{NDT} (RT_{NDT} initial + ΔRT_{NDT}) is used to index the material to the K_{IR} curve and, in turn, to set operating limits for the nuclear power plant which take into account the effects of irradiation on the reactor vessel materials.

SECTION 4
DESCRIPTION OF PROGRAM

Eight surveillance capsules for monitoring the effects of neutron exposure on the H. B. Robinson Unit 2 reactor pressure vessel core region material were inserted in the reactor vessel prior to initial plant startup. The eight capsules were positioned in the reactor vessel between the thermal shield and the vessel wall at locations shown in figure 4-1. The vertical center of the capsules is opposite the vertical center of the core.

Capsule T was removed after approximately 7.2 effective full power years of plant operation. This capsule, shown in figure 4-2, contained Charpy V-notch impact, tension, and IX-wedge opening loading (WOL) fracture mechanics specimens from the vessel intermediate shell plate W10201-6 and submerged arc weld metal representative of the core region of the reactor vessel and Charpy V-notch specimens from weld heat-affected zone (HAZ) material. The capsule also contained Charpy V-notch specimens from the 6-inch-thick ASTM correlation monitor material (A302 Grade B). The chemistry and heat treatment of the surveillance materials are presented in table 4-1. The chemical analyses reported in table 4-1 were obtained from unirradiated material used in the surveillance program. In addition, a chemical analysis was performed on two irradiated Charpy specimens from the weld metal and is also reported in table 4-1. The analysis of the irradiated weld metal indicates that the copper, nickel, and phosphorus contents are in good agreement with the unirradiated analysis.

Test specimens from the plate material were machined from the 1/4 thickness location of the plate. Test specimens represent material taken at least one plate thickness from the quenched end of the plate. All base metal Charpy V-notch specimens were oriented with the longitudinal axis of the specimen parallel to the principal rolling direction of the plate. Base metal tension specimens were oriented with the longitudinal axis of the specimen transverse to the rolling direction of the plate. Charpy V-notch and tension specimens from the weld metal were oriented with the longitudinal axis of the specimens transverse to the welding direction.

Capsule T contained dosimeter wires of pure copper, nickel, and aluminum-0.15 Wt% cobalt (cadmium-shielded and unshielded). In addition, cadmium-shielded dosimeters of Np^{237} and U^{238} were contained in the capsule. The test specimens served as iron dosimeters. Thermal monitors made from two low melting eutectic alloys sealed in quartz tubes were included in the capsule and were located as shown in figure 4-2. The two eutectic alloys and their melting points are as follows:

2.5% Ag, 97.5% Pb	Melting Point 579°F (304°C)
1.75% Ag, 0.75% Sn, 97.5% Pb	Melting Point 590°F (310°C)

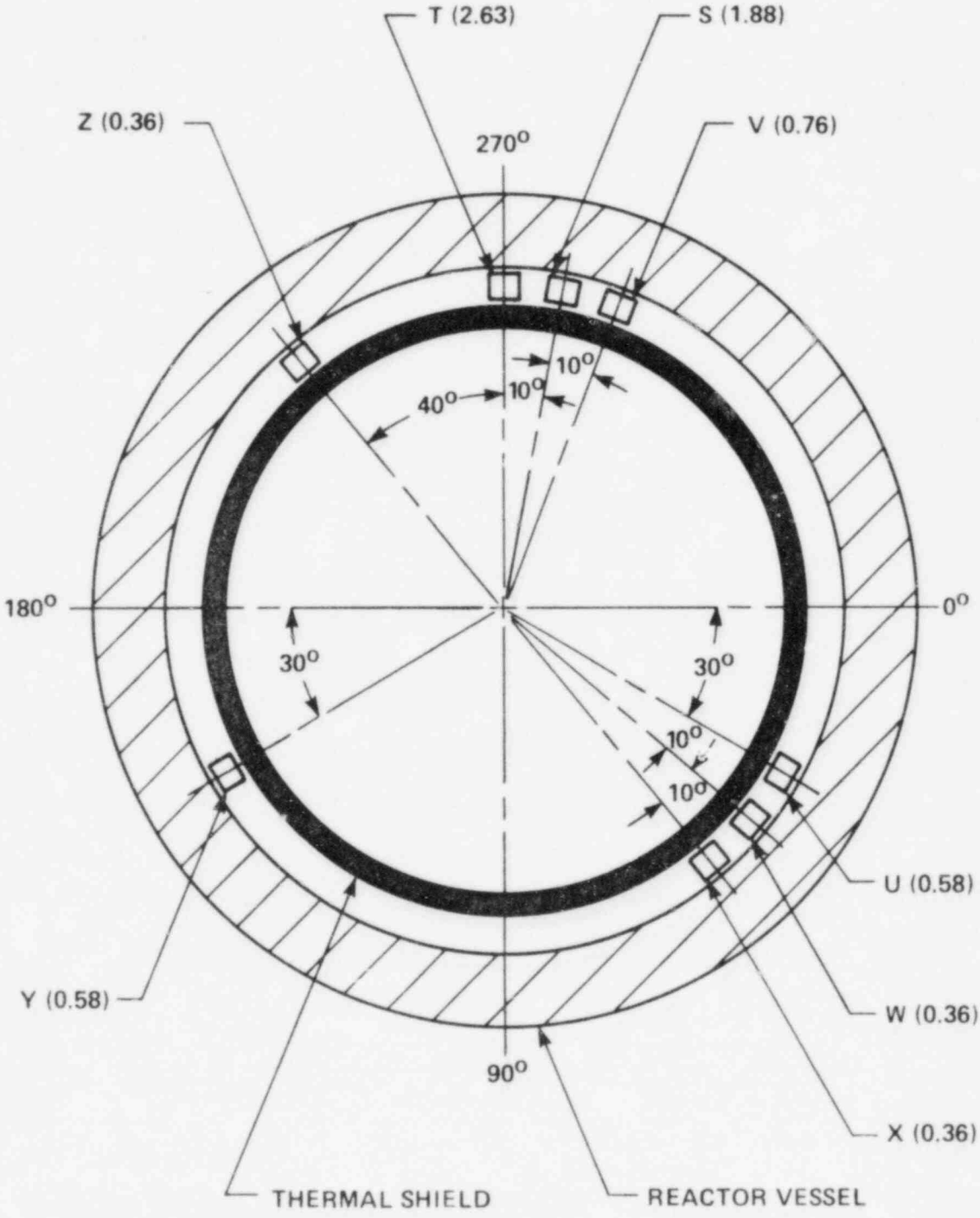

Figure 4-1. Arrangement of Surveillance Capsules in the H.B. Robinson Unit 2 Reactor Vessel

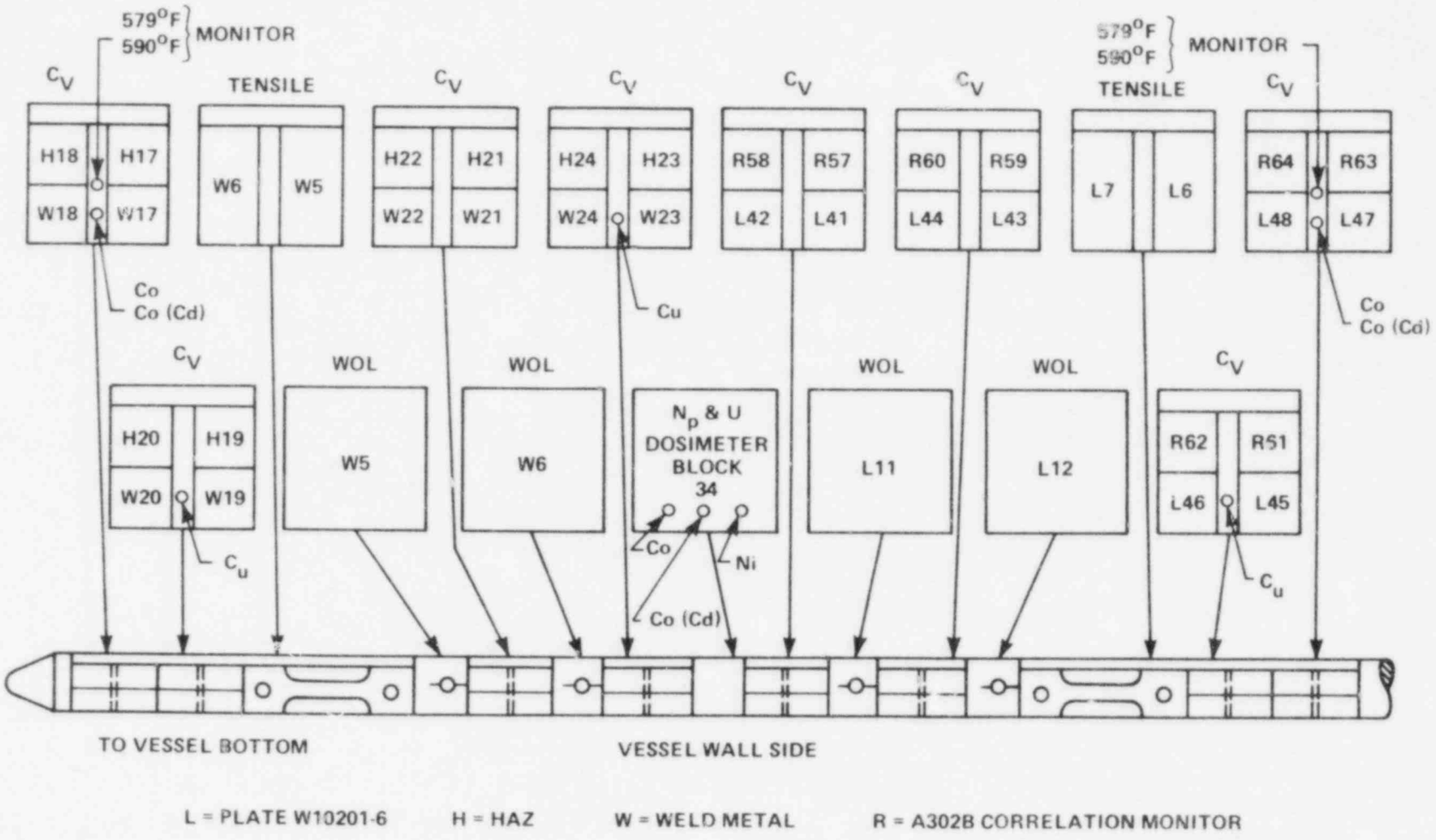

Figure 4-2. Arrangement of Specimens, Thermal Monitors, and Dosimeters in Capsule T

TABLE 4-1

CHEMICAL COMPOSITION AND HEAT TREATMENT OF MATERIAL FOR THE H. B. ROBINSON UNIT 2 REACTOR VESSEL SURVEILLANCE PROGRAM

Element	Chemical Composition (Wt%)						
	Plate W10201-4	Plate W10201-5	Plate W10201-6	Weld Metal	Weld Metal[a]		Correlation Monitor
					W21	W20	
C	0.19	0.20	0.19	0.16	0.075	—	0.24
Mn	1.35	1.29	1.32	0.98	1.36	—	1.34
P	0.007	0.010	0.010	0.021	0.026	—	0.011
S	0.019	0.021	0.015	0.014	0.033	—	0.023
Si	0.23	0.22	0.19	0.34	0.21	—	0.23
Mo	0.48	0.46	0.49	0.46	0.24	—	0.51
Cu	0.12	0.10	0.09	0.34	0.33	0.35	0.20
V	—	—	—	0.001	—	—	—
Ni	—	—	—	0.66	0.63	0.69	0.18
Cr	—	—	—	0.024	0.02	—	0.11
Co	—	—	—	—	0.007	—	—

Heat Treatment	
Plate W10201-4	1550°-1600°F, 4 hr, water quench
Plate W10201-5	1200°-1250°F, 4 hr, air cooled
Plate W10201-6	1125°-1175°F, 15 1/2 hr, furnace cooled to 600°F
Weld Metal	1125°-1175°F, 30 hr, furnace cooled to 600°F
Correlation Monitor	1650°F - 4 hr, water quenched 1200°F - 6 hr, air cooled

a. Analysis performed on irradiated Charpy specimens from Capsule T.

SECTION 5
TESTING OF SPECIMENS FROM CAPSULE T

5-1. OVERVIEW

The postirradiation mechanical testing of the Charpy V-notch and tension specimens was performed at the Westinghouse Research and Development Laboratory with consultation by Westinghouse Nuclear Energy Systems personnel. Testing was performed in accordance with 10CFR50, Appendixes G and H.

Upon receipt of the capsule at the laboratory, the specimens and spacer blocks were carefully removed, inspected for identification number, and checked against the master list in WCAP-7373 [1]. No discrepancies were found.

Examination of the two low-melting 304°C (579°F) and 310°C (590°F) eutectic alloys indicated no melting of either type of thermal monitor. Based on this examination, the maximum temperature to which the test specimens were exposed was less than 304°C (579°F).

The Charpy impact tests were performed on a Tinius-Olsen Model 74, 358-joule machine. The tup (striker) of the Charpy machine is instrumented with an Effects Technology Model 500 instrumentation system. With this system, load-time and energy-time signals can be recorded in addition to the standard measurement of Charpy energy (E_D). From the load-time curve, the load of general yielding (P_{GY}), the time to general yielding (t_{GY}), the maximum load (P_M), and the time to maximum load (t_M) can be determined. Under some test conditions, a sharp drop in load indicative of fast fracture was observed. The load at which fast fracture was initiated is identified as the fast fracture load (P_F), and the load at which fast fracture terminated is identified as the arrest load (P_A).

The energy at maximum load (E_M) was determined by comparing the energy-time record and the load-time record. The energy at maximum load is roughly equivalent to the energy required to initiate a crack in the specimen. Therefore, the propagation energy for the crack (E_p) is the difference between the total energy to fracture (E_D) and the energy at maximum load.

The yield stress (σ_y) is calculated from the three-point bend formula. The flow stress is calculated from the average of the yield and maximum loads, also using the three-point bend formula.

Percent shear was determined from postfracture photographs using the ratio-of-areas method in compliance with ASTM Specification A370-74. The lateral expansion was measured using a dial gage rig similar to that shown in the same specification.

Tension tests were performed on a 20,000-pound Instron, split-console test machine (Model 1115) per ASTM Specifications E8 and E21, and MHL Procedure 7604 Revision 2. All pull rods, grips, and pins were made of Inconel 718 hardened to R_C45. The upper pull rod was connected through a universal joint to improve axiality of loading. The tests were conducted at a constant crosshead speed of 0.05 inch per minute throughout the test.

Deflection measurements were made with a linear variable displacement transducer (LVDT) extensometer. The extensometer knife edges were spring-loaded to the specimen and operated through specimen failure. The extensometer gage length is 1.00 inch. The extensometer is rated as Class B-2 per ASTM E83.

Elevated test temperatures were obtained with a three-zone electric resistance split-tube furnace with a 9-inch hot zone. All tests were conducted in air.

Because of the difficulty in remotely attaching a thermocouple directly to the specimen, the following procedure was used to monitor specimen temperature. Chromel-alumel thermocouples were inserted in shallow holes in the center and each end of the gage section of a dummy specimen and in each grip. In test configuration, with a slight load on the specimen, a plot of specimen temperature versus upper and lower grip and controller temperatures was developed over the range room temperature to 550°F. The upper grip was used to control the furnace temperature. During the actual testing the grip temperatures were used to obtain desired specimen temperatures. Experiments indicated that this method is accurate to plus or minus 2°F.

The yield load, ultimate load, fracture load, total elongation, and uniform elongation were determined directly from the load-extension curve. The yield strength, ultimate strength, and fracture strength were calculated using the original cross-sectional area. The final diameter and final gage length were determined from postfracture photographs. The fracture area used to calculate the fracture stress (true stress at fracture) and percent reduction in area was computed using the final diameter measurement.

5-2. CHARPY V-NOTCH IMPACT TEST RESULTS

The toughness results from Charpy V-notch impact tests performed on the various surveillance materials in Capsule T after irradiation to 4.11×10^{19} n/cm^2 are presented in tables 5-1 through 5-3 and figures 5-1 through 5-4. Instrumented Charpy impact test results for the various materials are shown in tables 5-4 through 5-6. A summary of the surveillance test results is presented in table 5-7. The fractured surfaces of the impact specimens are shown in figures 5-5 through 5-7.

TABLE 5-1

CHARPY IMPACT DATA FOR H. B. ROBINSON UNIT 2
REACTOR VESSEL SHELL PLATE W10201-6
(IRRADIATED AT 4.11 x 10^{19} n/cm^2)

Sample No.	Temperature		Impact Energy		Lateral Expansion		Shear (%)
	°C	°F	J	ft lb	mm	mils	
L48	26	78	30.0	22.0	0.55	21.5	33
L41	38	100	46.0	34.0	0.72	28.5	40
L46	66	150	65.0	48.0	1.09	43.0	60
L43	79	175	106.5	78.5	1.63	64.0	80
L47	93	200	116.0	85.5	1.99	78.5	92
L45	121	250	148.0	109.0	1.99	78.5	100
L44	177	350	139.0	102.5	1.88	74.0	100

TABLE 5-2

CHARPY IMPACT DATA FOR H. B. ROBINSON UNIT 2
REACTOR VESSEL WELD METAL AND HAZ MATERIAL
(IRRADIATED AT 4.11 x 10^{19} n/cm^2)

Sample No.	Temperature		Impact Energy		Lateral Expansion		Shear (%)
	°C	°F	J	ft lb	mm	mils	
Weld Metal							
W17	79	175	19.0	14.0	0.24	9.5	15
W22	93	200	32.0	23.5	0.46	18.0	35
W18	93	200	23.0	17.0	0.38	15.0	15
W20	107	225	87.0	64.0	1.22	48.0	92
W19	121	250	52.0	38.5	0.75	29.5	40
W23	135	275	70.0	51.5	1.00	39.5	90
W24	149	300	82.0	60.5	1.26	49.5	98
HAZ Metal							
H17	93	200	117.5	86.5	1.61	63.5	98
H24	149	300	132.0	97.5	1.96	77.0	100

Irradiation of Charpy V-notch specimens from the intermediate shell course plate W10201-6 to 4.11 x 10^{19} n/cm^2 resulted in a 41-joule (30 ft lb) and 68-joule (50 ft lb) transition temperature increase of 42°C (75°F) and 44°C (80°F), respectively, when compared with unirradiated values as shown in figure 5-1. The upper shelf energy of plate W10201-6 decreased by 12 joules (9 ft lb)

TABLE 5-3

CHARPY IMPACT DATA FOR THE ASTM A302B
CORRELATION MONITOR MATERIAL
(IRRADIATED AT 4.11×10^{19} n/cm^2)

Sample No.	Temperature		Impact Energy		Lateral Expansion		Shear (%)
	°C	°F	J	ft lb	mm	mils	
R63	26	78	37.5	27.5	0.56	22.0	15
R59	26	78	17.0	12.5	0.25	10.0	10
R62	66	150	20.5	15.0	0.28	11.0	35
R64	93	200	32.5	24.0	0.53	21.0	45
R58	107	225	46.0	34.0	0.81	32.0	96
R60	121	250	49.5	36.5	0.88	34.5	99
R61	149	300	46.0	34.0	0.81	32.0	100
R57	177	350	55.0	40.5	0.93	36.5	100

after irradiation to 4.11×10^{19} n/cm^2. A comparison of these results with prior results after irradiation to 3.69×10^{18} n/cm^2, shown in table 5-8, indicates that the increased neutron fluence produced an additional 30° to 34°C increase in transition temperature and an additional reduction in the upper shelf energy level of 4 joules.

Weld metal specimens irradiated to 4.11×10^{19} n/cm^2 as shown in figure 5-2 resulted in a 41- and 68- joule transition temperature increase of 158°C. A comparison of these results with prior test results on the weld metal irradiated to 5.84×10^{18} n/cm^2 is shown in table 5-8. This comparison shows that the 41- and 68-joule transition temperature increases for the 4.11×10^{19} n/cm^2 irradiation were 61°C and 39°C higher, respectively, than the results for irradiation at 5.84×10^{18} n/cm^2. Two Charpy impact tests were performed on the weld HAZ metal specimens as shown in figure 5-3 in the vicinity of the upper shelf to confirm that the HAZ metal exhibits an upper shelf energy in excess of 68 joules. The remaining HAZ specimens are being held in abeyance at the request of the Carolina Power and Light Company. Reconstituting the weld portion of the unbroken specimens and performing additional Charpy tests on the weld metal are currently under consideration.

ASTM A302B correlation monitor material irradiated to 4.11×10^{19} n/cm^2 showed a 41-joule transition temperature increase of 84°C when compared with unirradiated results as shown in figure 5-4. Specimens from this material were oriented transverse to the major rolling direction of the plate and exhibited upper shelf energy levels less than 68 joules in both the unirradiated and irradiated conditions. A 4-joule decrease in shelf energy resulted from irradiation to 4.11×10^{19} n/cm^2. A comparison of the 41-joule transition temperature increase with prior results from irradiations to 3.69×10^{18} and 5.84×10^{18} n/cm^2 as shown in table 5-8 indicates that irradiation to 4.11×10^{19} n/cm^2 produced an additional increase in transition temperature of 45°C.

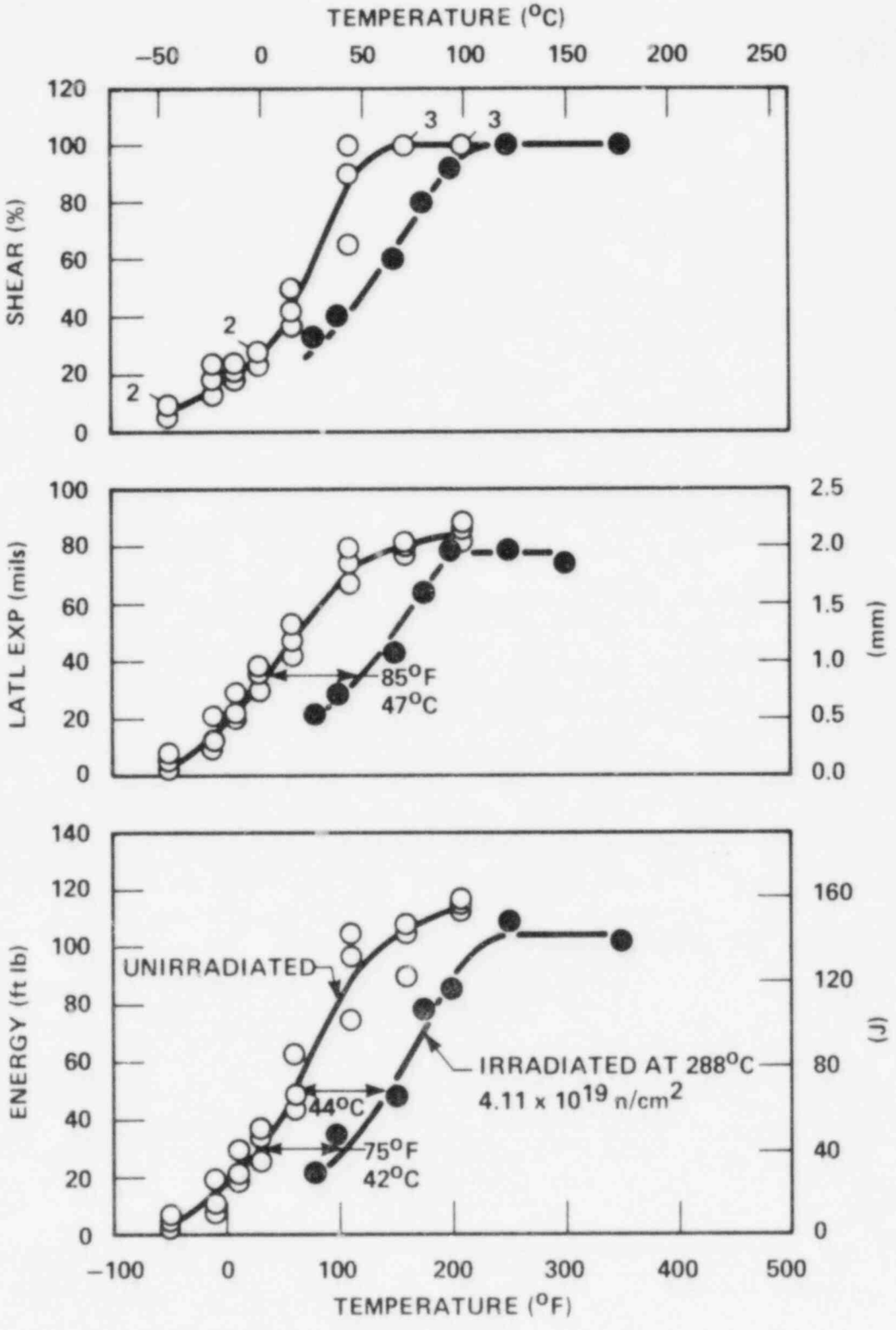

Figure 5-1. Charpy V-Notch Impact Data for H.B. Robinson Unit 2 Reactor Vessel Shell Plate W10201-6

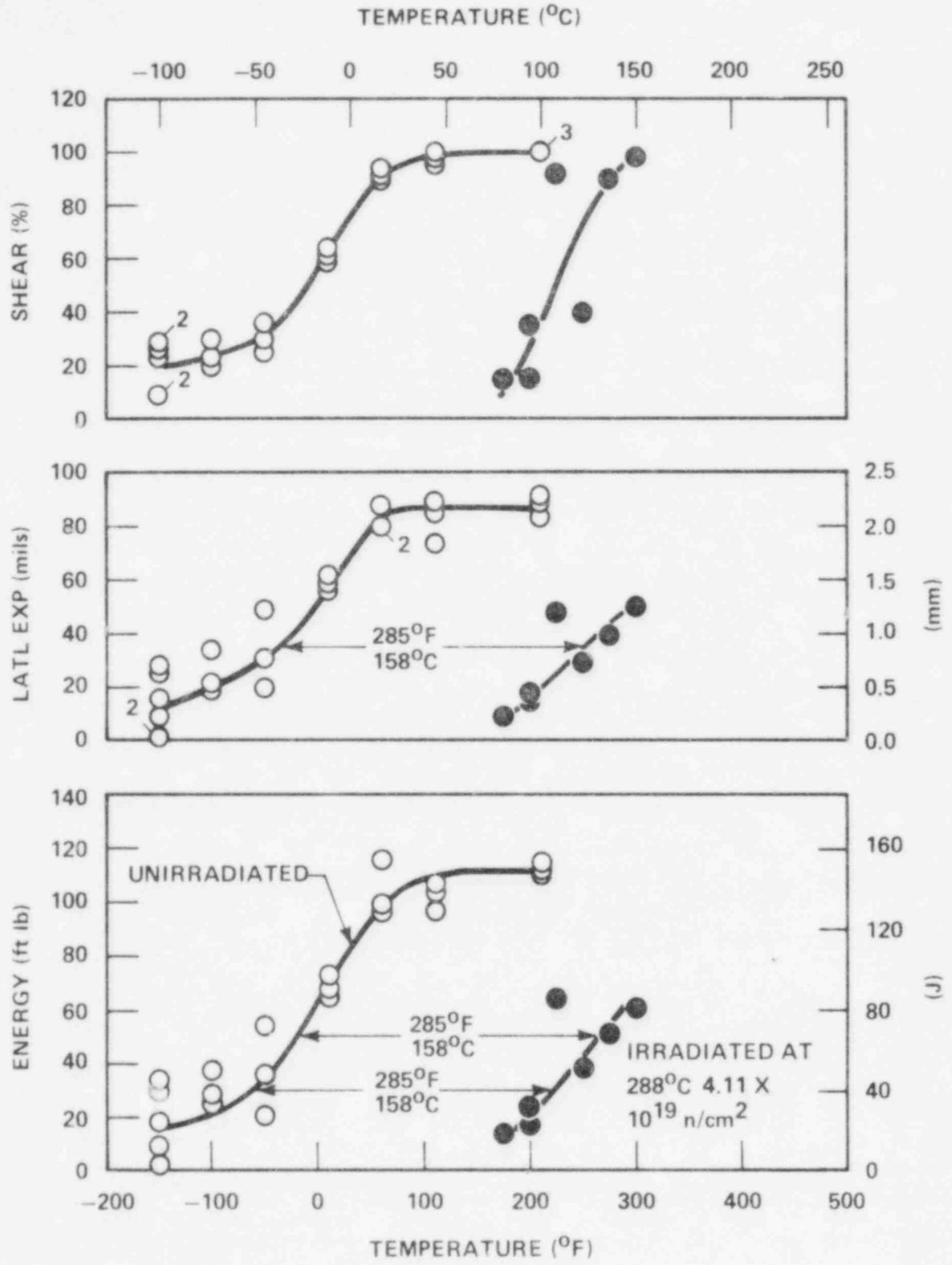

Figure 5-2. Charpy V-Notch Impact Data for H.B. Robinson Unit 2 Reactor Vessel Weld Metal

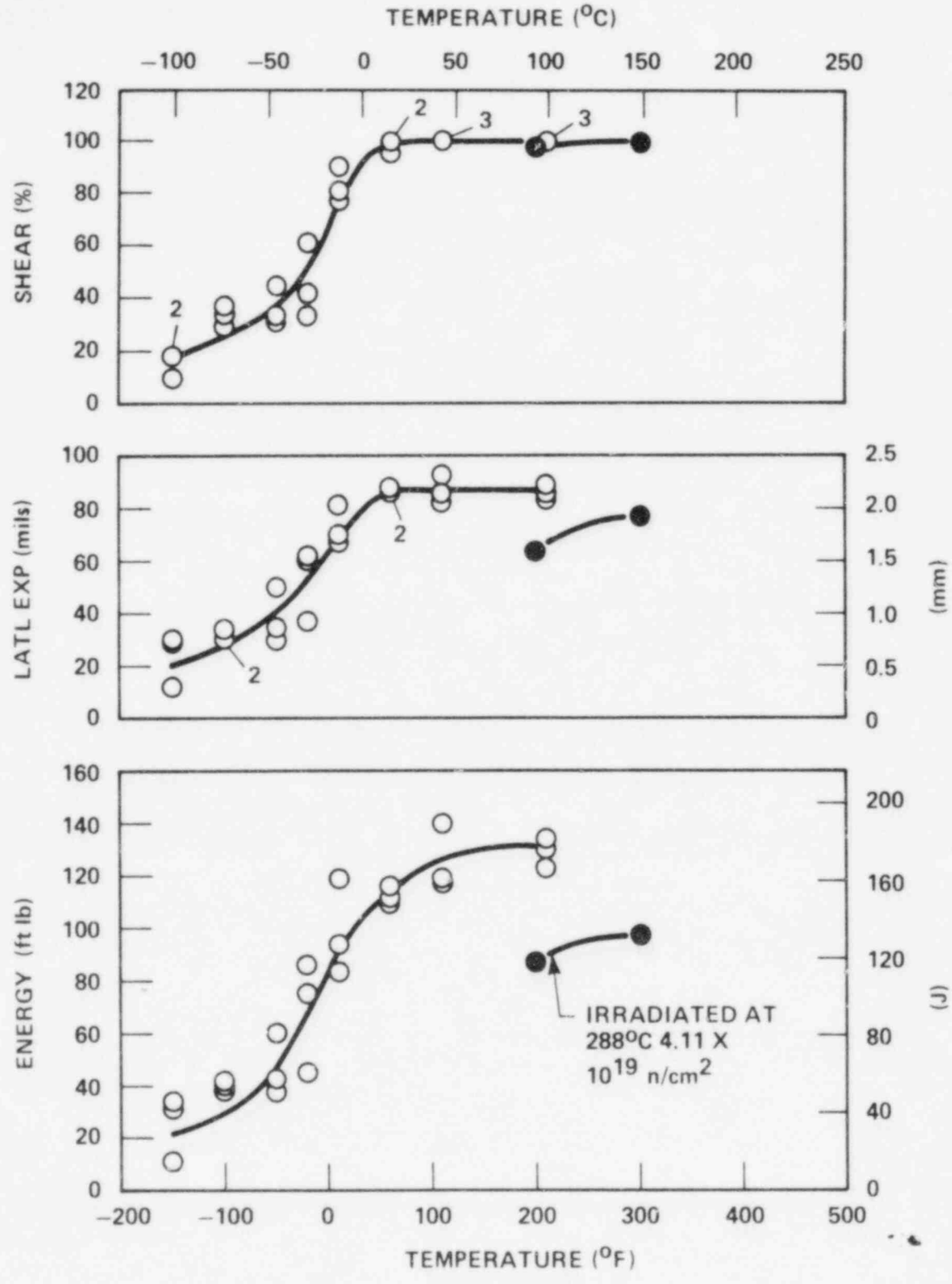

Figure 5-3. Charpy V-Notch Impact Data for H.B. Robinson Unit 2 Reactor Vessel Weld HAZ Material

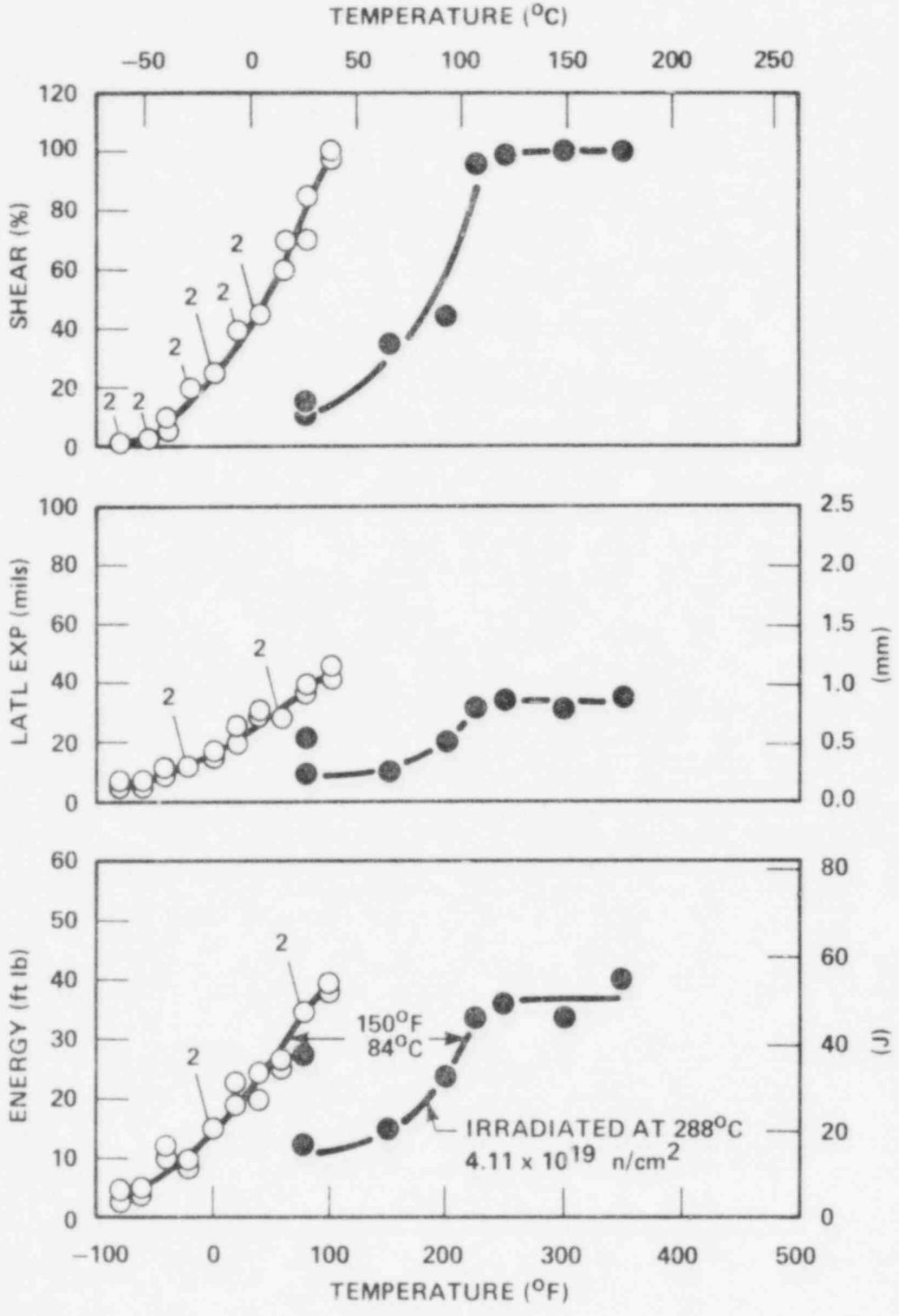

Figure 5-4. Charpy V-Notch Impact Data for H.B. Robinson Unit 2 ASTM A302B Correlation Monitor Material (Transverse Orientation)

TABLE 5-4

INSTRUMENTED CHARPY IMPACT TEST RESULTS FOR H. B. ROBINSON UNIT 2 REACTOR VESSEL SHELL PLATE W10201-6

Sample No.	Test Temp (°C)	Charpy Energy (J)	Normalized Energies			Yield Load (N)	Time to Yield (μs)	Maximum Load (N)	Time to Maximum (μs)	Fracture Load (N)	Arrest Load (N)	Yield Stress (MPa)	Flow Stress (MPa)
			Charpy Ed/A (kJ/m^2)	Maximum Em/A (kJ/m^2)	Prop Ep/A (kJ/m^2)								
L48	26	30.0	373										
L41	38	46.0	576	350	226	12300	100	16000	450	16000	5400	630	728
L46	66	65.0	813	530	284	11700	95	16000	670	16000	7500	604	713
L43	79	106.5	1330	468	862	11600	125	15800	605	15700	12500	595	703
L47	93	116.0	1449	532	917	12600	165	16300	660			650	745
L45	121	148.0	1847	667	1180	11400	100	16800	810			585	725
L44	177	139.0	1737	603	1134	9100	100	14200	860			466	587

TABLE 5-5

INSTRUMENTED CHARPY IMPACT TEST RESULTS FOR H. B. ROBINSON UNIT 2 WELD METAL AND HAZ MATERIAL

Sample No.	Test Temp (°C)	Charpy Energy (J)	Normalized Energies			Yield Load (N)	Time to Yield (μs)	Maximum Load (N)	Time to Maximum (μs)	Fracture Load (N)	Arrest Load (N)	Yield Stress (MPa)	Flow Stress (MPa)
			Charpy Ed/A (kJ/m^2)	Maximum Em/A (kJ/m^2)	Prop Ep/A (kJ/m^2)								
Weld Metal													
W17	79	19.0	237	153	84	15200	105	17000	205	17300	100	781	828
W22	93	32.0	398	308	90	14700	100	17900	360	17900	0	757	840
W18	93	23.0	288	216	72	15200	105	17900	265	17900	100	781	850
W20	107	87.0	1085	448	636	14200	105	18500	500			732	841
W19	121	52.0	652	398	254	15000	105	18600	440	17700	3000	770	863
W23	135	70.0	873	387	486	15800	115	18800	430			813	891
W24	149	82.0	1025	356	669	13900	105	18100	415			717	824
HAZ Metal													
H17	93	117.5	1466	542	924	14800	105	18700	590			763	863
H24	149	132.0	1652	531	1121	13100	125	17900	605			676	799

TABLE 5-6

INSTRUMENTED CHARPY IMPACT TEST RESULTS FOR ASTM A302B CORRELATION MONITOR MATERIAL

Sample No.	Test Temp (°C)	Charpy Energy (J)	Normalized Energies			Yield Load (N)	Time to Yield (μs)	Maximum Load (N)	Time to Maximum (μs)	Fracture Load (N)	Arrest Load (N)	Yield Stress (MPa)	Flow Stress (MPa)
			Charpy Ed/A (kJ/m^2)	Maximum Em/A (kJ/m^2)	Prop Ep/A (kJ/m^2)								
R59	26	17.0	212	174	38	15500	110	16600	230			797	825
R63	26	37.5	466	223	243	16200	100	17800	260	17800	0	833	875
R62	66	20.5	254	157	97	15000	100	16600	210	16600	1700	770	811
R64	93	32.5	407	227	179	14700	125	17200	280	16900	6000	758	822
R58	107	46.0	576	206	370	13300	100	16100	275			684	755
R60	121	49.5	619	221	398	14400	105	17200	275			739	813
R61	149	46.0	576	198	378	13700	105	16600	265			705	780
R57	177	55.0	686	192	494	12800	105	16200	265			661	748

TABLE 5-7

THE EFFECT OF 288°C IRRADIATION AT 4.11 x 10^{19} n/cm^2 (E > 1.0 MeV) ON THE NOTCH TOUGHNESS PROPERTIES OF H. B. ROBINSON UNIT 2 REACTOR VESSEL MATERIALS

Material	Transition Temperature												Δ Transition Temperature						Average Energy Absorption at Full Shear					
	Unirradiated						Irradiated																	
	50 ft lb 68 J		30 ft lb 41 J		35 mils 9 mm		50 ft lb 68 J		30 ft lb 41 J		35 mils 9 mm		50 ft lb 68 J		30 ft lb 41 J		35 mils 9 mm		Unirradiated		Irradiated		Δ Energy	
	(°C)	(°F)	(°C)	(°F)	(°C)	(°F)	(°C)	(°F)	(°C)	(°F)	(°C)	(°F)	(°C)	(°F)	(°C)	(°F)	(°C)	(°F)	(J)	(ft lb)	(J)	(ft lb)	(J)	(ft lb)
Plate W10201-6	16	60	-1	30	2	35	60	140	41	105	49	120	44	80	42	75	47	85	154	114	142	105	12	9
Weld Metal	-29	-20	-51	-60	-37	-35	129	265	107	225	121	250	158	285	158	285	158	285	152	112	–	–	–	–
HAZ Metal	-43	-45	-73	-100	-57	-70	–	–	–	–	–	–	–	–	–	–	–	–	178	131	132	97	46	34
Correlation Monitor	–	–	18	65	21	70	–	–	102	215	–	–	–	–	84	150	–	–	54	40	50	37	4	3

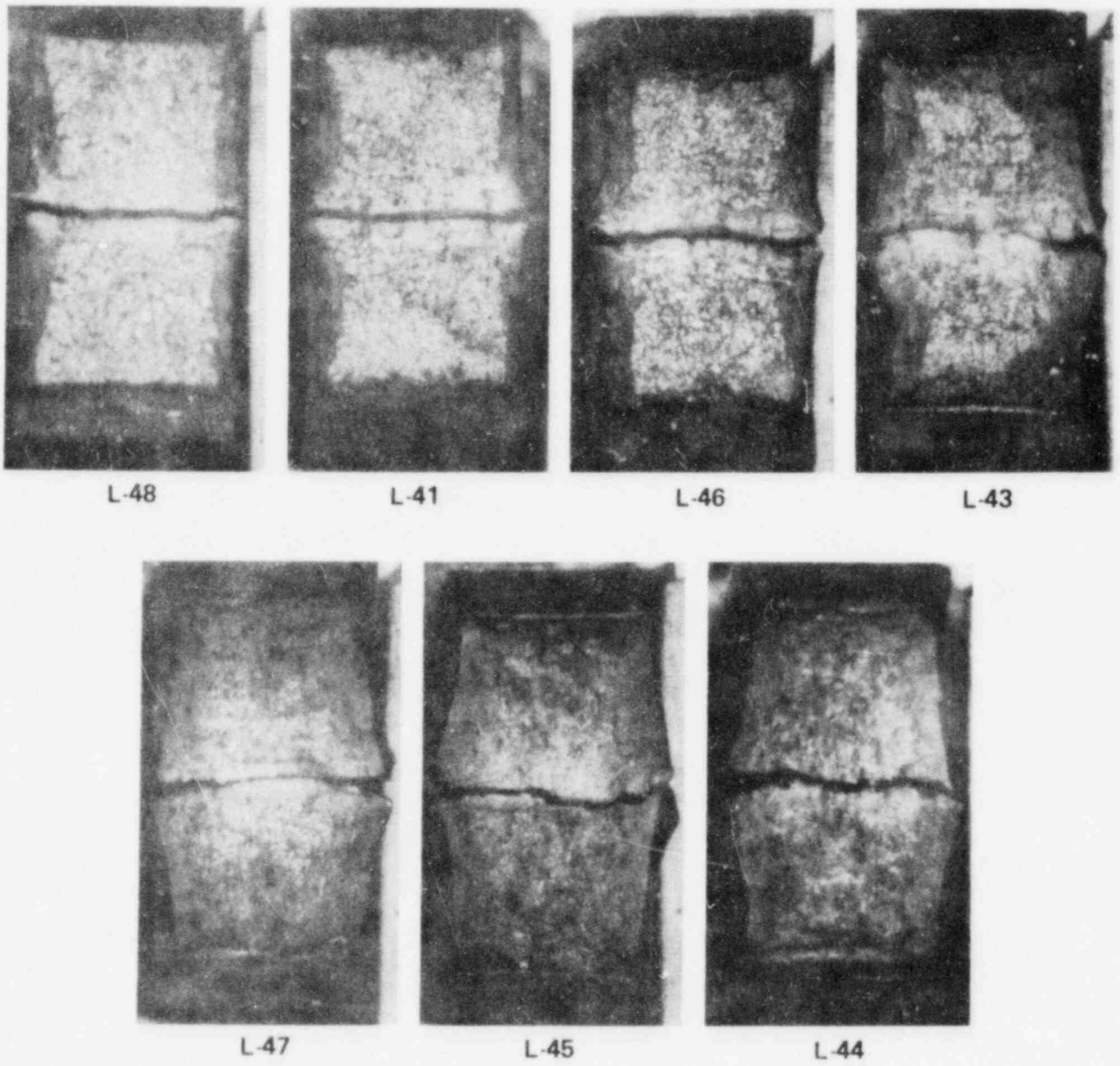

Figure 5-5. Charpy Impact Specimen Fracture Surfaces for H.B. Robinson Unit 2 Reactor Vessel Shell Plate W10201-6

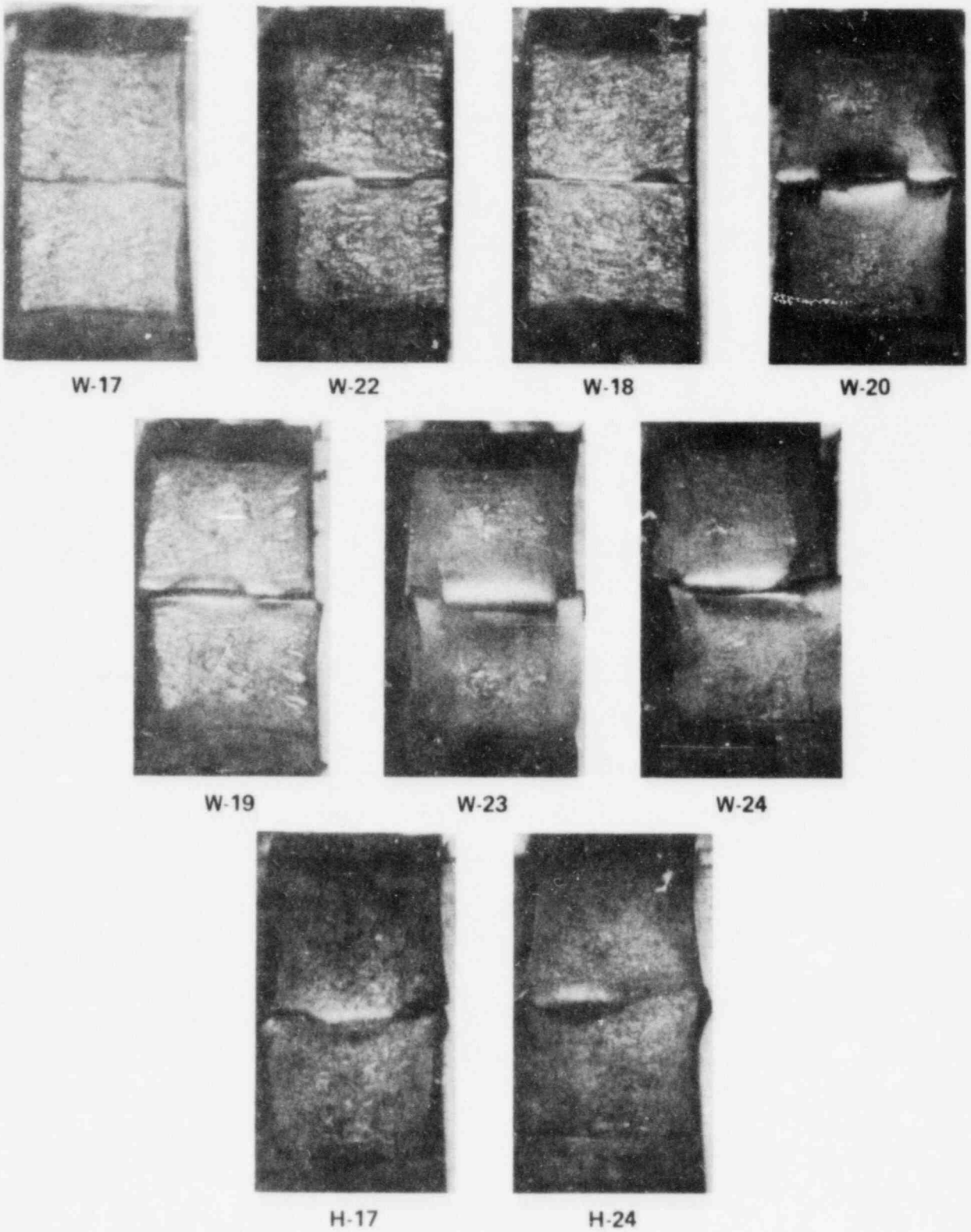

Figure 5-6. Charpy Impact Specimen Fracture Surfaces for H.B. Robinson Unit 2 Weld Metal and HAZ Metal

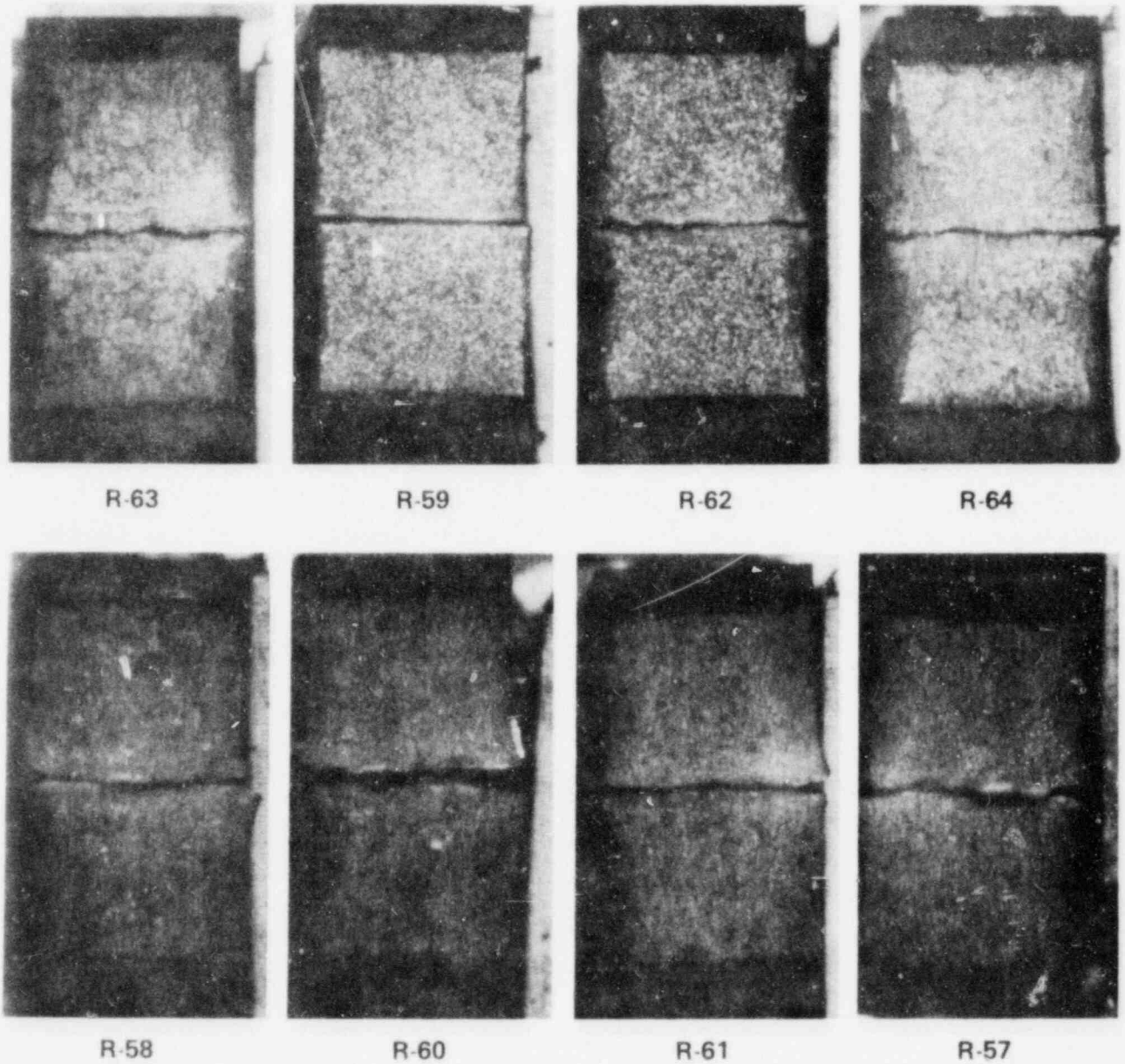

Figure 5-7. Charpy Impact Specimen Fracture Surfaces for H.B. Robinson Unit 2 ASTM A302B Correlation Monitor Material

TABLE 5-8

SUMMARY OF H. B. ROBINSON UNIT 2 REACTOR VESSEL
SURVEILLANCE CAPSULE CHARPY IMPACT TEST RESULTS

Material	Fluence (10^{19} n/cm^2)	68 J 50 ft lb Trans. Temp Increase (°C)	(°F)	41 J 30 ft lb Trans. Temp Increase (°C)	(°F)	Decrease in Upper Shelf Energy (J)	(ft lb)
Plate W10201-4	0.369	25	45	17	30	11	8
Plate W10201-5	0.369	22	40	11	20	18	13
Plate W10201-5	0.584	28	50	25	45	0	0
Plate W10201-6	0.369	14	25	8	15	8	6
Plate W10201-6	4.11	44	80	42	75	12	9
Weld Metal	0.584	119	215	97	175	57	42
Weld Metal	4.11	158	285	158	285	—	—
HAZ Metal	0.584	47	85	36	65	47	35
HAZ Metal	4.11	—	—	—	—	46	34
Correlation Monitor	0.369	—	—	39	70	4	3
Correlation Monitor	0.584	—	—	39	70	4	3
Correlation Monitor	4.11	—	—	84	150	4	3

The fracture appearance of each irradiated Charpy specimen from the various materials is shown in figures 5-5 through 5-7. An increasing ductile or tougher appearance with increasing temperature can be noted for each of the materials.

Figure 5-8 shows a comparison of the 41-joule transition temperature increase for the H. B. Robinson Unit 2 surveillance materials with predicted increases using the methods of NRC Regulatory Guide 1.99 Revision 1. This comparison shows that all the materials exhibited 41-joule transition temperature increases lower than would be predicted by the Guide. This behavior is consistent with the results from other reactor vessel surveillance capsules evaluated as part of this EPRI program. Based on the surveillance capsule test results to date, it can be concluded that the H. B. Robinson Unit 2 surveillance materials are not as sensitive to radiation as predicted by the Guide.

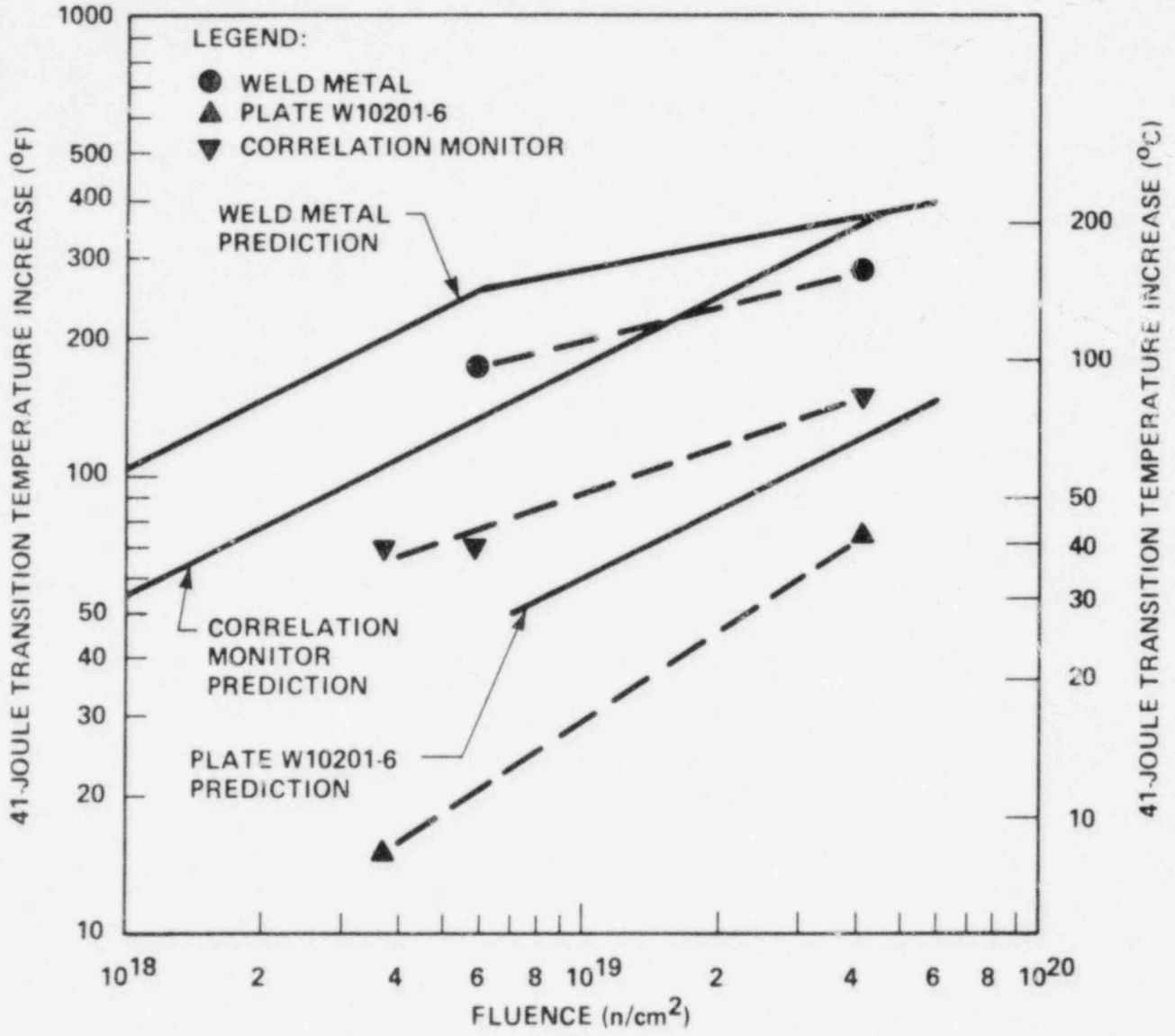

Figure 5-8. Comparison of Actual Versus Predicted 41-Joule Transition Temperature Increase for H.B. Robinson Unit 2 Reactor Vessel Materials Using the Prediction Methods of Regulatory Guide 1.99 Revision 1

5-3. TENSION TEST RESULTS

The results of tension tests performed on shell plate W10201-6 and weld metal are shown in table 5-9 and figures 5-9 and 5-10, respectively. An increase in 0.2 percent yield strength of approximately 12 and 27 ksi (82.7 and 186.2 MPa) was exhibited by the plate and weld metal, respectively. These increases indicate that the weld metal is more sensitive to radiation than the base metal plate which is consistent with transition temperature increases observed for these materials. Photographs of the fractured tension specimens for each material are shown in figure 5-11. A typical stress-strain curve for the tension specimens is shown in figure 5-12.

5-4. WEDGE OPENING LOADING TESTS

Wedge opening loading (WOL) fracture mechanics specimens which were contained in the surveillance capsule have been stored at the Westinghouse Research Laboratory; they will be tested and reported on later.

TABLE 5-9

TENSILE PROPERTIES FOR H. B. ROBINSON UNIT 2 REACTOR VESSEL MATERIALS IRRADIATED TO 4.11×10^{19} n/cm^2

Sample No.	Material	Test Temp °C (°F)	0.2% Yield Strength MPa (ksi)	Ultimate Strength MPa (ksi)	Fracture Load N (kip)	Fracture Stress MPa (ksi)	Fracture Strength MPa (ksi)	Uniform Elongation (%)	Total Elongation (%)	Reduction in Area (%)
L7	Plate W10201-6	93 (200)	389 (56.4)	527 (76.4)	12,800 (2.88)	980 (141.5)	405 (58.7)	13.8	23.7	59
L6	Plate W10201-6	288 (550)	337 (48.9)	530 (76.8)	13,900 (3.12)	850 (124.0)	438 (63.6)	13.2	21.5	49
W5	Weld Metal	135 (275)	611 (88.6)	692 (100.4)	15,800 (3.55)	1370 (198.2)	499 (72.3)	8.7	17.8	64
W6	Weld Metal	288 (550)	597 (86.6)	702 (101.9)	18,700 (4.20)	1290 (187.2)	590 (85.6)	8.4	16.2	54

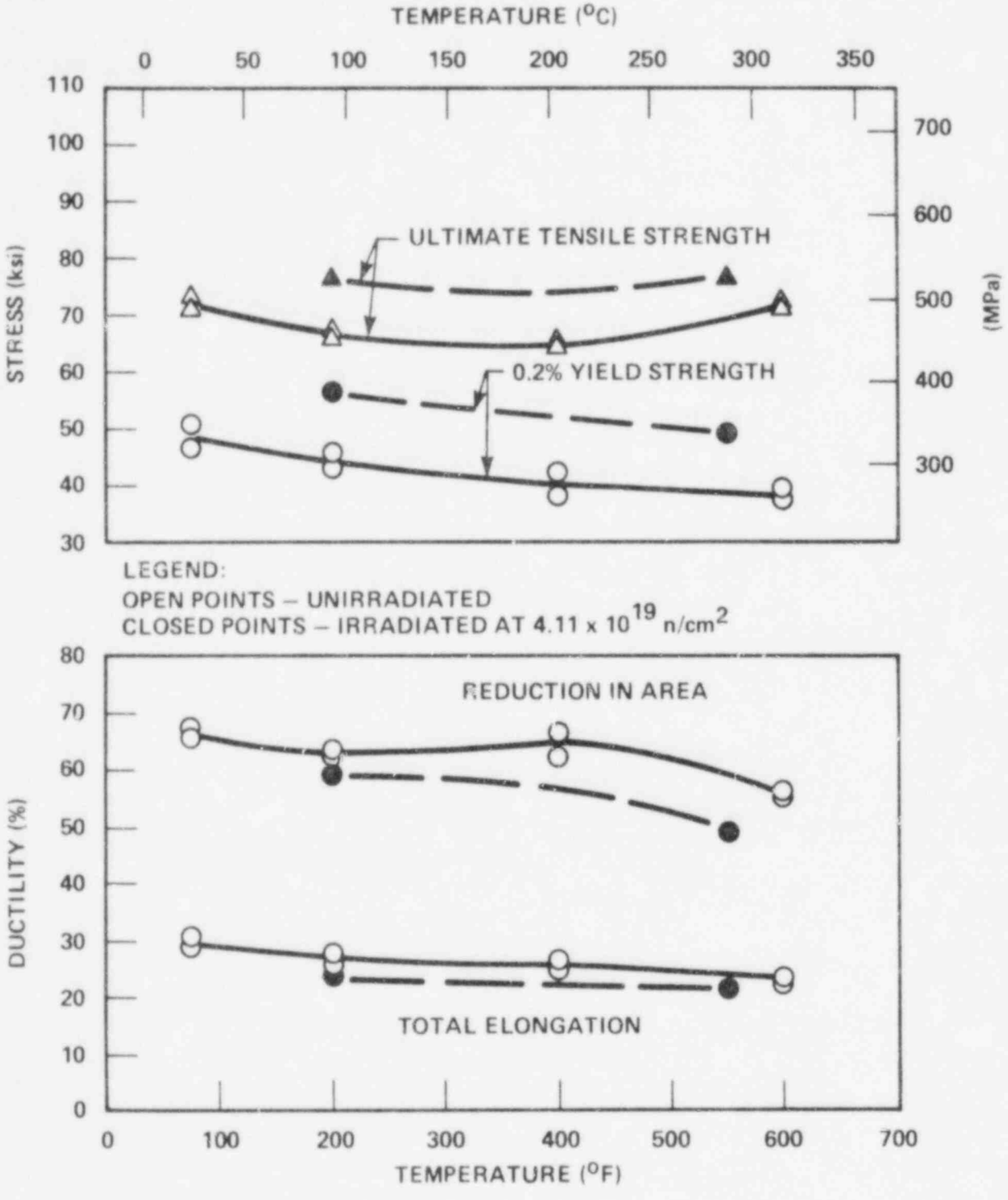

Figure 5-9. Tensile Properties for H.B. Robinson Unit 2 Reactor Vessel Shell Plate W10201-6

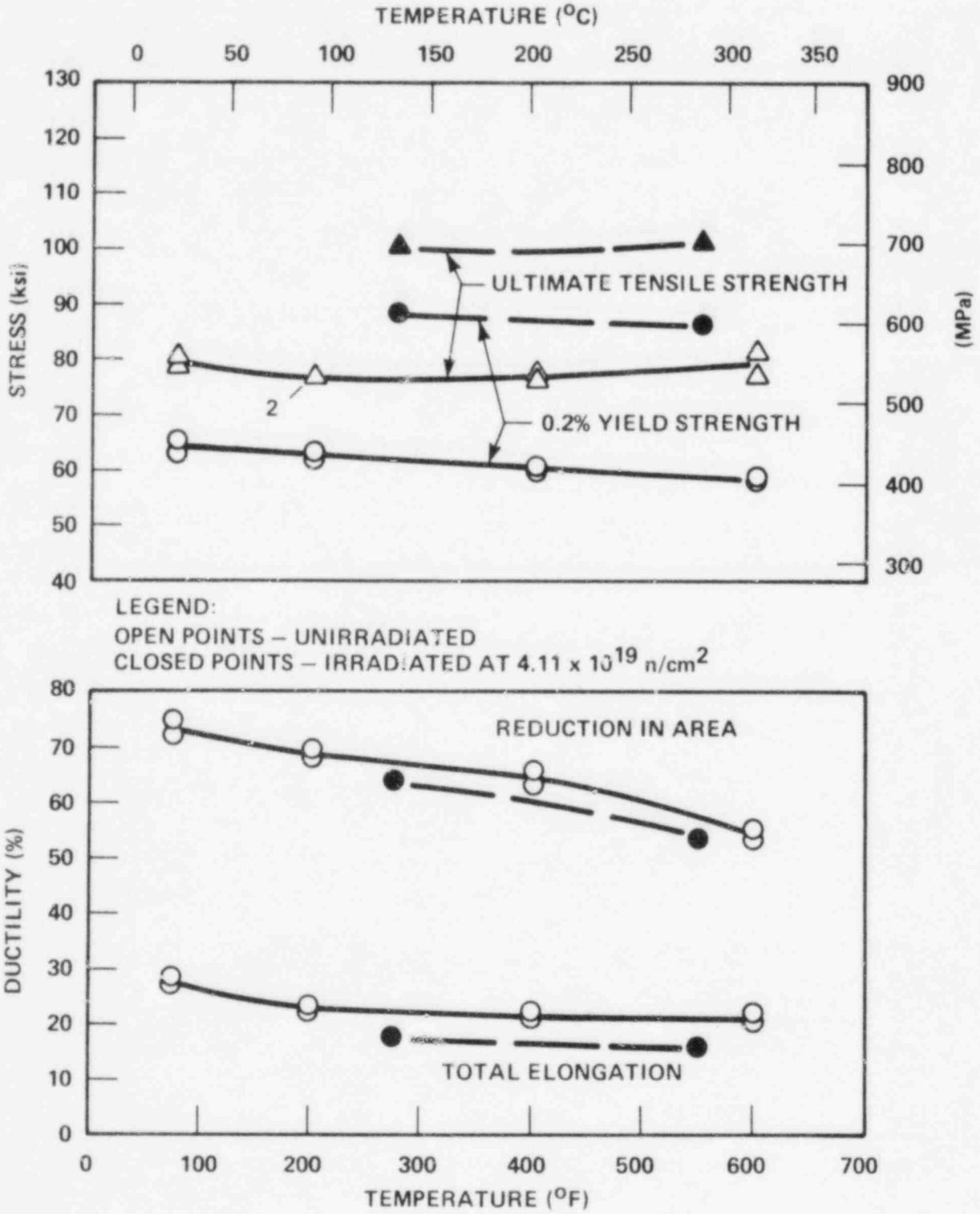

Figure 5-10. Tensile Properties for H.B. Robinson Unit 2 Reactor Vessel Weld Metal

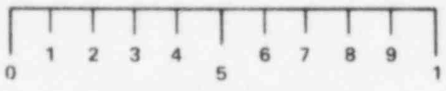

SPECIMEN L-7 TESTED AT 200°F

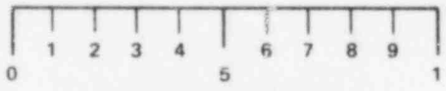

SPECIMEN L-6 TESTED AT 550°F

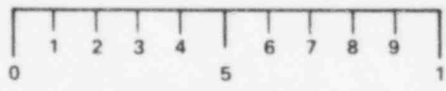

SPECIMEN W-5 TESTED AT 275°F

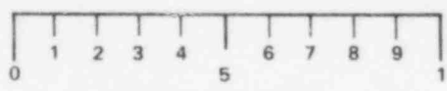

SPECIMEN W-6 TESTED AT 550°F

Figure 5-11. Fractured Tension Specimens from H.B. Robinson Unit 2 Shell Plate W10201-6 and Weld Metal

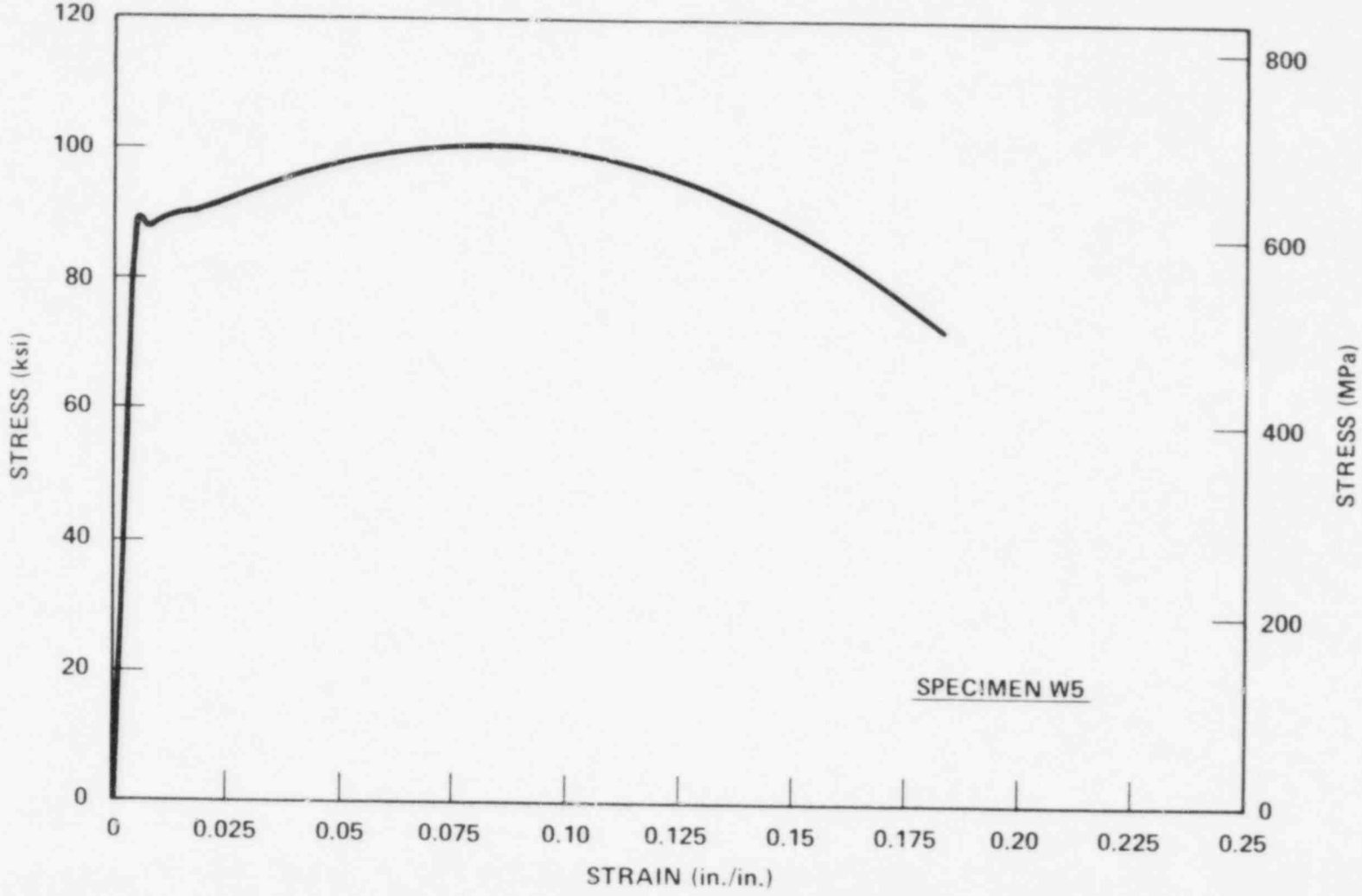

Figure 5-12. Typical Stress - Strain Curve for Tension Specimens

SECTION 6
RADIATION ANALYSIS AND NEUTRON DOSIMETRY

6-1. INTRODUCTION

Knowledge of the neutron environment within the pressure vessel - surveillance capsule geometry is required as an integral part of LWR pressure vessel surveillance programs for two reasons. First, in the interpretation of radiation-induced property changes observed in materials test specimens, the neutron environment (fluence, flux) to which the test specimens were exposed must be known. Second, in relating the changes observed in the test specimens to the present and future condition of the reactor pressure vessel, a relationship between the environment at various positions within the reactor vessel and that experienced by the test specimens must be established. The former requirement is normally met by employing a combination of rigorous analytical techniques and measurements obtained with passive neutron flux monitors contained in each of the surveillance capsules. The latter information is derived solely from analysis.

This section describes a discrete ordinates Sn transport analysis performed for the H. B. Robinson Unit 2 reactor to determine the fast neutron ($E > 1.0$ MeV) flux and fluence as well as the neutron energy spectra within the reactor vessel and surveillance capsules and, in turn, to develop lead factors for use in relating neutron exposure of the pressure vessel to that of the surveillance capsules. Based on spectrum-averaged reaction cross sections derived from this calculation, the analysis of the neutron dosimetry contained in Capsule T is discussed.

6-2. DISCRETE ORDINATES ANALYSIS

A plan view of the H. B. Robinson Unit 2 reactor geometry at the core midplane is shown in figure 6-1. Since the reactor exhibits 1/8th core symmetry, only a 45-degree sector is depicted. Eight irradiaton capsules attached to the thermal shield are included in the design to constitute the reactor vessel surveillance program. The location of each of the eight surveillance capsules relative to the reactor core cardinal axes is also depicted in figure 6-1.

A plan view of a single surveillance capsule attached to the thermal shield is shown in figure 6-2. The stainless steel specimen container is 1-inch square and approximately 63 inches in height. The containers are positioned axially such that the specimens are centered on the core midplane, thus spanning the central 5.25 feet of the 12-foot-high reactor core.

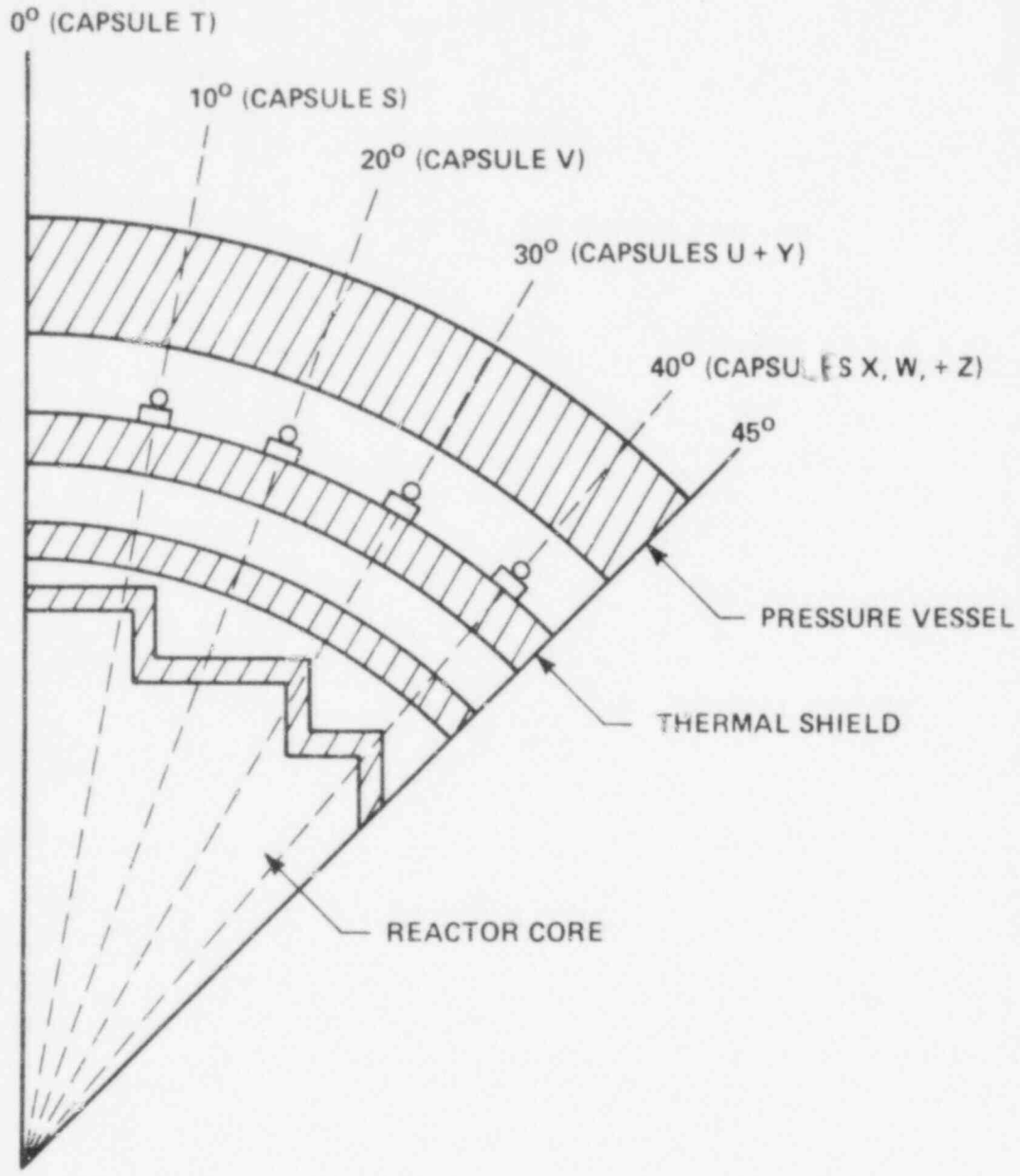

Figure 6-1. R, Theta Reactor Geometry

From a neutronic standpoint, the surveillance capsule structures are significant. In fact, as is shown later, they have a marked impact on the distributions of neutron flux and energy spectra in the water annulus between the thermal shield and the reactor vessel. Thus, in order to properly ascertain the neutron environment at the test specimen locations, the capsules themselves must be included in the analytical model. Use of at least a two-dimensional computation is, therefore, mandatory.

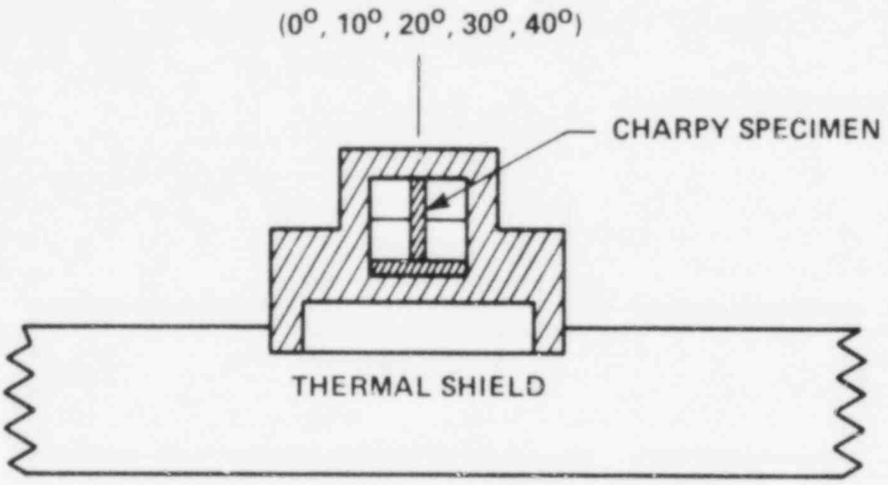

Figure 6-2. Plan View of a Reactor Vessel Surveillance Capsule

In the analysis of the neutron environment within the H. B. Robinson Unit 2 reactor geometry, predictions of neutron flux magnitude and energy spectra were made with the DOT[5] two-dimensional discrete ordinates code. The radial and azimuthal distributions were obtained from an R, θ computation wherein the geometry shown in figures 6-1 and 6-2 was described in the analytical model. In addition to the R, θ computation, a second calculation in R, Z geometry was also carried out to obtain relative axial variations of neutron flux throughout the geometry of interest. In the R, Z analysis the reactor core was treated as an equivalent volume cylinder and, of course, the surveillance capsules were not included in the model.

Both the R, θ and the R, Z analyses employed 21 neutron energy groups, an S_8 angular quadrature, and a P_1 cross-section expansion. The cross sections were generated via the Westinghouse GAMB1T[6] code system with broad group processing by the APPROPOS[7] and ANISN[8] codes. The energy group structure used in the analysis is listed in table 6-I.

A key input parameter in the analysis of the integrated fast neutron exposure of the reactor vessel is the core power distribution. For this analysis, power distributions representative of time-averaged conditions derived from statistical studies of long-term operation of Westinghouse 3-loop plants were employed. These input distributions include rod-by-rod spatial variations for all peripheral fuel assemblies.

It should be noted that this particular power distribution is intended to produce accurate end-of-life neutron exposure levels for the pressure vessel. As such, the calculation is indeed representative of an average neutron flux and small (plus or minus 15 to 20 percent) deviations from cycle to cycle are to be expected.

TABLE 6-1
21 GROUP ENERGY STRUCTURE

Group	Lower Energy (MeV)
1	7.79[a]
2	6.07
3	4.72
4	3.68
5	2.87
6	2.23
7	1.74
8	1.35
9	1.05
10	0.821
11	0.388
12	0.111
13	4.09×10^{-2}
14	1.50×10^{-2}
15	5.53×10^{-3}
16	5.83×10^{-4}
17	7.89×10^{-5}
18	1.07×10^{-5}
19	1.86×10^{-6}
20	3.00×10^{-7}
21	0.0

a. Upper energy of group 1 is 10.0 MeV

Having the results of the R,θ and R,Z calculations, three-dimensional variations of neutron flux may be approximated by assuming that the following relation holds for the applicable regions of the reactor.

$$\phi(R,Z,\theta,E_g) = \phi(R,\theta,E_g)\, F(Z,E_g) \qquad (6\text{-}1)$$

where

$\phi(R,Z,\theta,E_g)$ = neutron flux at point R,Z,θ within energy group g

$\phi(R,\theta,E_g)$ = neutron flux at point R,θ within energy group g obtained from the R,θ calculation

6-3. NEUTRON DOSIMETRY

The passive neutron flux monitors included in the H. B. Robinson Unit 2 surveillance program are listed in table 6-2. The first five reactions in table 6-2 are used as fast neutron monitors to relate neutron fluence (E > 1.0 MeV) to measured materials properties changes. To properly account for burnout of the product isotope generated by fast neutron reactions, it is necessary to also determine the magnitude of the thermal neutron flux at the monitor location. Therefore, bare and cadmium-covered cobalt-aluminum monitors were also included.

The relative locations of the various monitors within the surveillance capsules are shown in figure 4-2. The nickel, copper, and cobalt-aluminum monitors, in wire form, are placed in holes drilled in spacers at several axial levels within the capsules. The iron monitors are obtained by drilling samples from selected Charpy test specimens. The cadmium-shielded neptunium and uranium fission monitors are accommodated within the dosimeter block located near the center of the capsule.

The use of passive monitors such as those listed in table 6-2 does not yield a direct measure of the energy-dependent flux level at the point of interest. Rather, the activation or fission process is a measure of the integrated effect that the time- and energy-dependent neutron flux has on the target material over the course of the irradiation period. An accurate assessment of the average

TABLE 6-2

NUCLEAR PARAMETERS FOR NEUTRON FLUX MONITORS

Monitor Material	Reaction of Interest	Target Weight Fraction	Response Range	Product Half-Life	Fission Yield (%)
Copper	$Cu^{63}(n,\alpha)Co^{60}$	0.6917	$E > 4.7$ MeV	5.27 yr	
Iron	$Fe^{54}(n,p)Mn^{54}$	0.0585	$E > 1.0$ MeV	314 d	
Nickel	$Ni^{58}(n,p)Co^{68}$	0.6777	$E > 1.0$ MeV	71.4 d	
Uranium-238[a]	$U^{238}(n,f)Cs^{137}$	1.0	$E > 0.4$ MeV	30.2 yr	6.3
Neptunium-237[a]	$Np^{237}(n,f)Cs^{137}$	1.0	$E > 0.08$ MeV	30.2 yr	6.5
Cobalt-Aluminum[a]	$Co^{59}(n,\gamma)Co^{60}$	0.0015	0.4 eV $< E < 0.015$ MeV	5.27 yr	
Cobalt-Aluminum	$Co^{59}(n,\gamma)Co^{60}$	0.0015	$E < 0.0015$ MeV	5.27 yr	

a. Denotes that monitor is cadmium shielded

neutron flux level incident on the various monitors may be derived from the activation measurements only if the irradiation parameters are well known. In particular, the following variables are of interest:

- The operating history of the reactor
- The energy response of the monitor
- The neutron energy spectrum at the monitor location
- The physical characteristics of the monitor

The analysis of the passive monitors and subsequent derivation of the average neutron flux requires completion of two procedures. First, the disintegration rate of product isotope per unit mass of monitor must be determined. Second, in order to define a suitable spectrum averaged reaction cross section, the neutron energy spectrum at the monitor location must be calculated.

The specific activity of each of the monitors is determined using established ASTM procedures.[9,10,11,12,13] Following sample preparation, the activity of each monitor is determined by means of a lithium-drifted germanium, Ge(Li), gamma spectrometer. The overall standard deviation of the measured data is a function of the precision of sample weighing, the uncertainty in counting, and the acceptable error in detector calibration. For the samples removed from H. B. Robinson Unit 2, the overall 2σ deviation in the measured data is determined to be plus or minus 10 percent. The neutron energy spectra are determined analytically using the method described in paragraph 6-1.

Having the measured activity of the monitors and the neutron energy spectra at the locations of interest, the calculation of the neutron flux proceeds as follows.

The reactor product activity in the monitor is expressed as

$$R = \frac{N_o}{A} f_i \gamma \int_E \sigma(E)\ \phi\ (E)\ dE \sum_{j=1}^{N} \frac{P_j}{P_{max}} (1 - e^{-\lambda t_j})\ e^{-\lambda t_d} \qquad (6\text{-}2)$$

where

R	=	induced product activity
N_o	=	Avogadro's number
A	=	atomic weight of the target isotope
f_i	=	weight fraction of the target isotope in the target material
γ	=	number of product atoms produced per reaction
$\sigma(E)$	=	energy-dependent reaction cross section
$\phi(E)$	=	energy-dependent neutron flux at the monitor location with the reactor at full power
P_j	=	average core power level during irradiation period j
P_{max}	=	maximum or reference core power level
λ	=	decay constant of the product isotope
t_j	=	length of irradiation period j
t_d	=	decay time following irradiation period j

Because neutron flux distributions are calculated using multigroup transport methods and, further, because the prime interest is in the fast neutron flux above 1.0 MeV, spectrum-averaged reaction cross sections are defined such that the integral term in equation (6-2) is replaced by the following relation.

$$\int_E \sigma(E)\ \phi(E)\ dE = \bar{\sigma}\ \phi\ (E > 1.0\ MeV)$$

where

$$\bar{\sigma} = \frac{\int_0^\infty \sigma(E)\ \phi(E)\ dE}{\int_{1.0\ MeV}^\infty \phi(E)\ dE} = \frac{\sum_{g=1}^{N} \sigma_g\ \phi_g}{\sum_{g=g_{1.0\ MeV}}^{N} \phi_g}$$

Thus, equation (6-2) is rewritten

$$R = \frac{N_o}{A} f_i \gamma \bar{\sigma} \phi (E > 1.0 \text{ MeV}) \sum_{j=1}^{N} \frac{P_j}{P_{max}} (1 - e^{-\lambda t_j}) e^{-\lambda t_d}$$

or, solving for the neutron flux,

$$\phi (E > 1.0 \text{ MeV}) = \frac{R}{\frac{N_o}{A} f_i \gamma \bar{\sigma} \sum_{j=1}^{N} \frac{P_j}{P_{max}} (1 - e^{-\lambda t_j}) e^{-\lambda t_d}} \quad (6\text{-}3)$$

The total fluence above 1.0 MeV is then given by

$$\Phi (E > 1.0 \text{ MeV}) = \phi (E > 1.0 \text{ MeV}) \sum_{j=1}^{N} \frac{P_j}{P_{max}} t_j$$

where

$\sum_{j=1}^{N} \frac{P_j}{P_{max}} t_j$ = total effective full power seconds of reactor operation up to the time of capsule removal

An assessment of the thermal neutron flux levels within the surveillance capsules is obtained from the bare and cadmium-covered $Co^{59}(n,\gamma)Co^{60}$ data by means of cadmium ratios and the use of a 37-barn 2,200 m/sec cross section. Thus,

$$\phi_{Th} = \frac{R_{bare}\left\{\frac{D-1}{D}\right\}}{\frac{N_o}{A} f_i \gamma \sigma \sum_{j=1}^{N} \frac{P_j}{P_{max}} (1-e^{-\lambda t_j}) e^{-\lambda t_d}} \quad (6\text{-}4)$$

where D is defined as $R_{bare}/R_{Cd\ covered}$.

6-4. TRANSPORT ANALYSIS RESULTS

Results of the S_n transport calculations for the H. B. Robinson Unit 2 reactor are summarized in figures 6-3 through 6-7 and in tables 6-3 through 6-5. In figure 6-3, the calculated maximum neutron flux levels at the surveillance capsule centerline, pressure vessel inner radius, 1/4 thickness location, and 3/4 thickness location are presented as a function of aximuthal angle. The influence of the surveillance capsules on the fast neutron flux distribution is clearly evident. In figures 6-4, the radial distribution of maximum fast neutron flux (E > 1.0 MeV) through the thickness of the

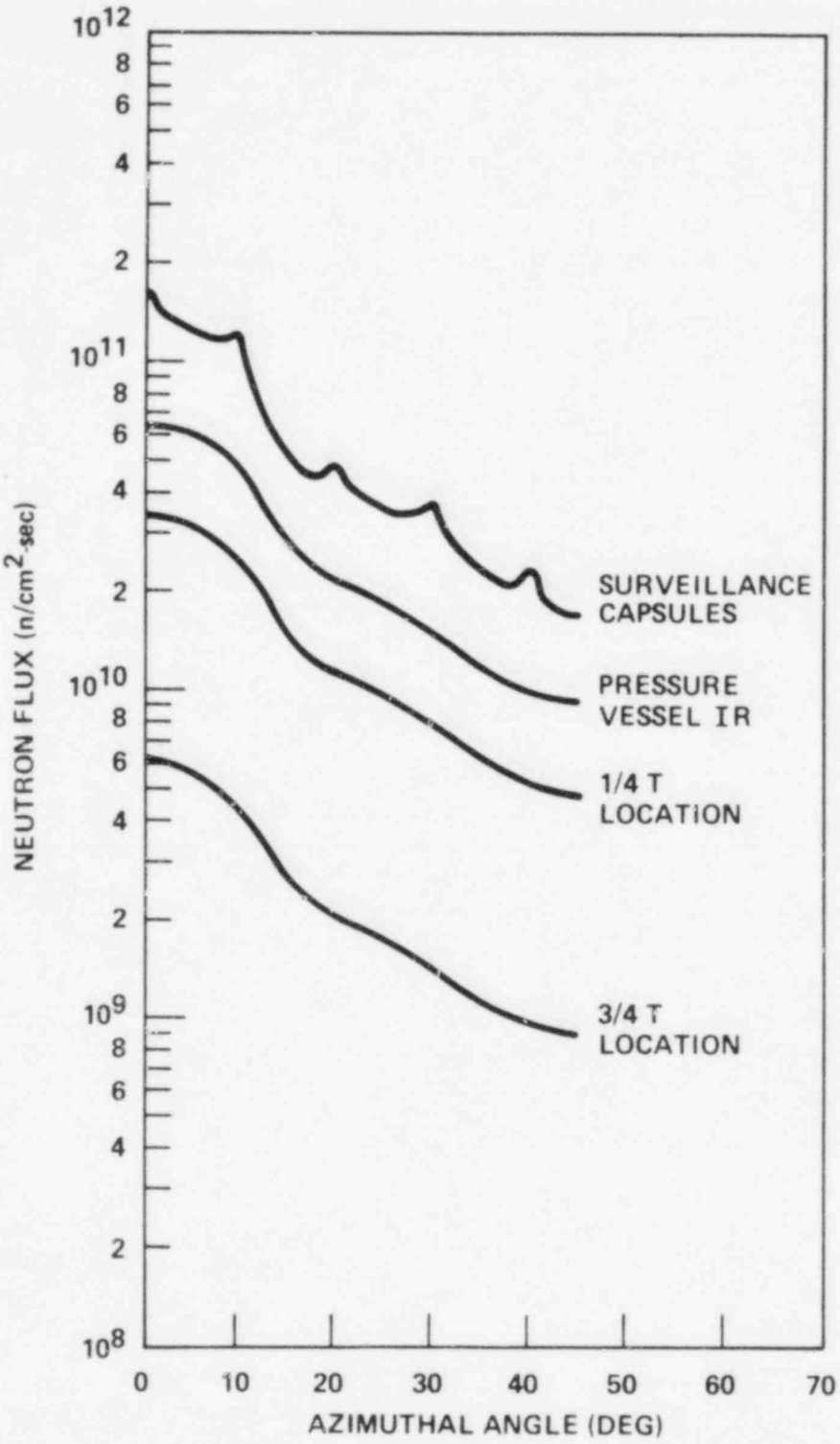

Figure 6-3. Calculated Azimuthal Distribution of Maximum Fast Neutron Flux ($E < 1.0$ MeV) Within the Pressure Vessel - Surveillance Capsule Geometry

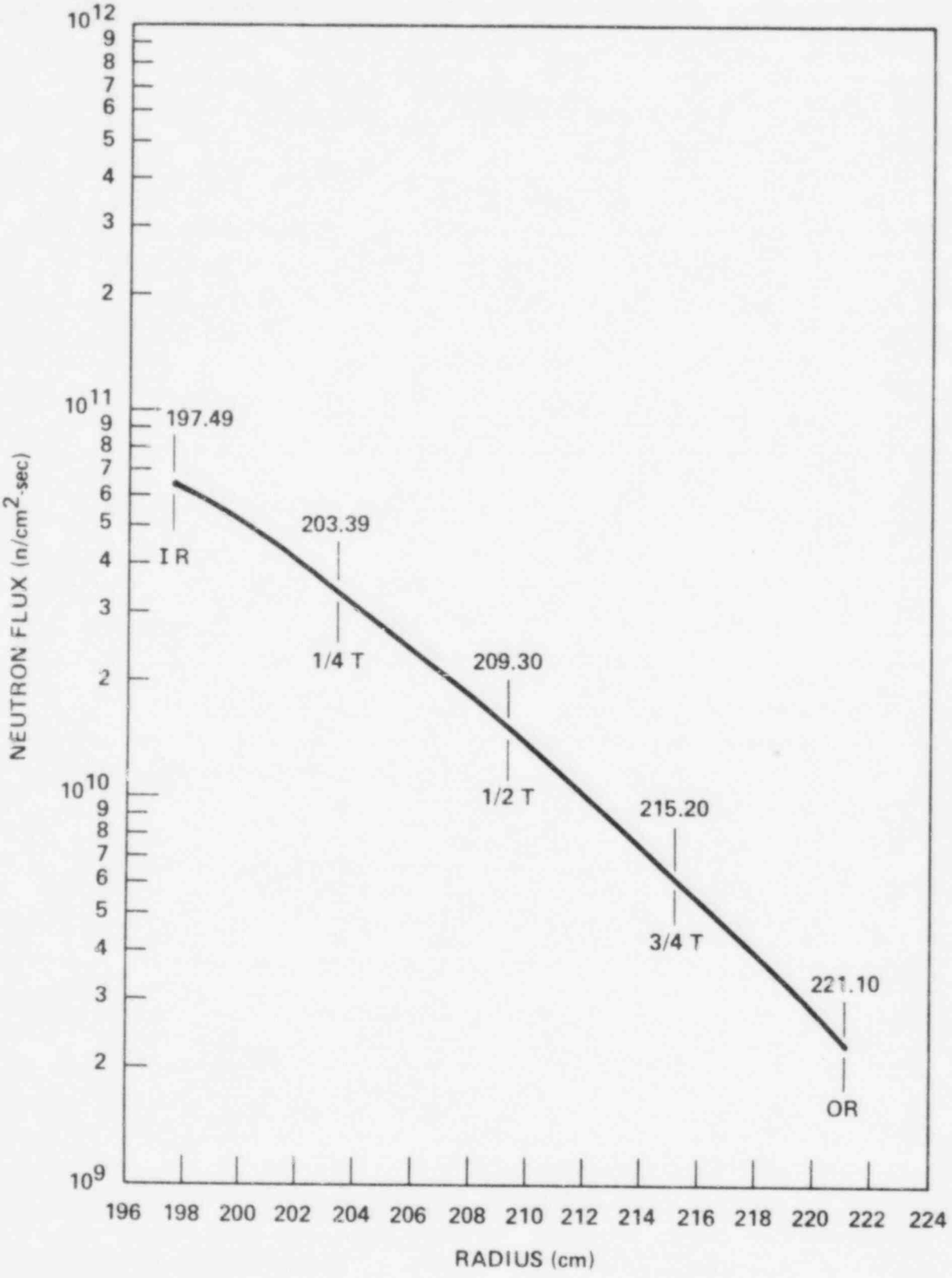

Figure 6-4. Calculated Radial Distribution of Maximum Fast Neutron Flux ($E > 1.0$ MeV) Within the Pressure Vessel

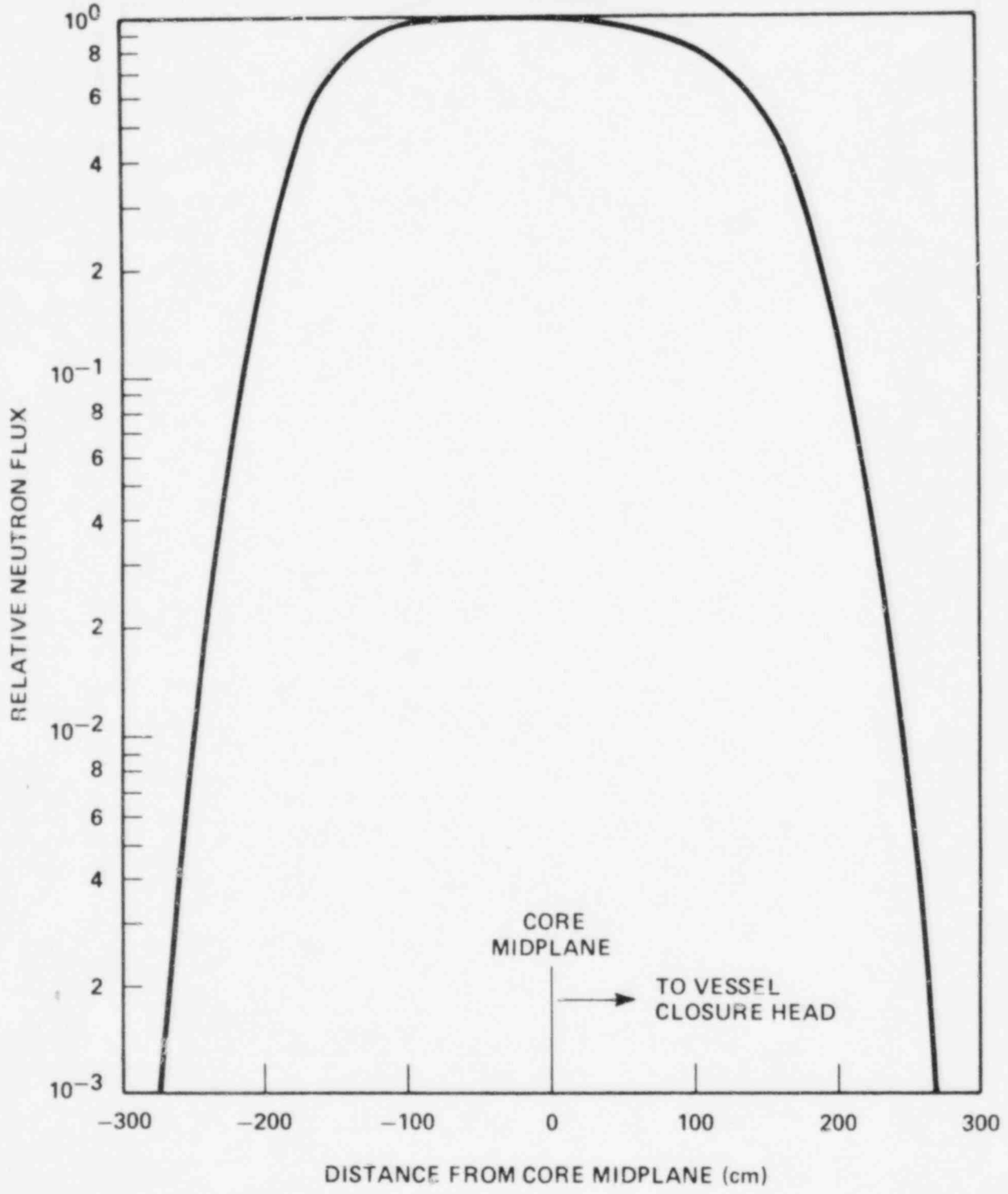

Figure 6-5. Relative Axial Variation of Fast Neutron Flux ($E > 1.0$ MeV) Within the Pressure Vessel

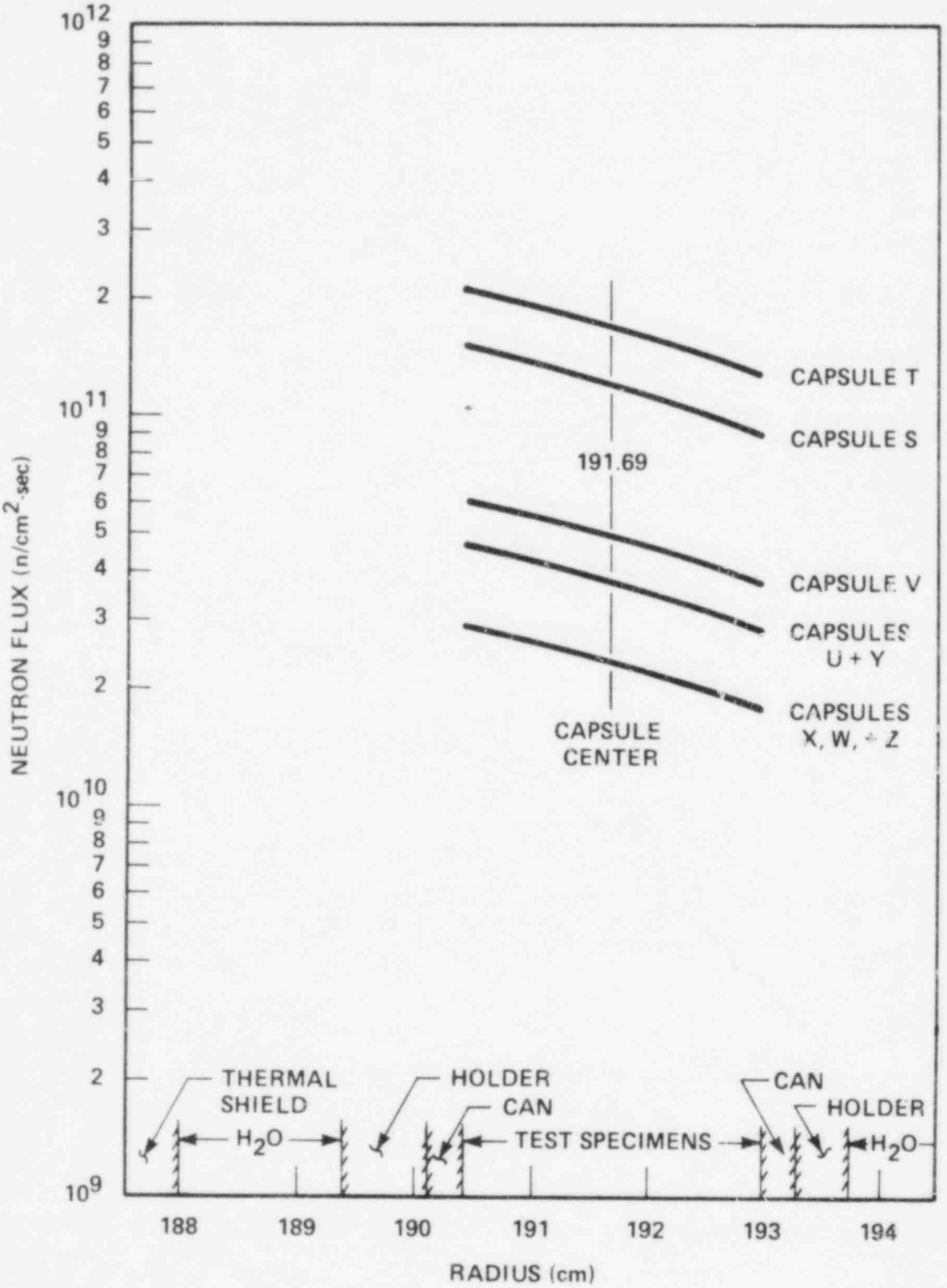

Figure 6-6. Calculated Radial Distribution of Maximum Fast Neutron Flux ($E > 1.0$ MeV) Within the Surveillance Capsules

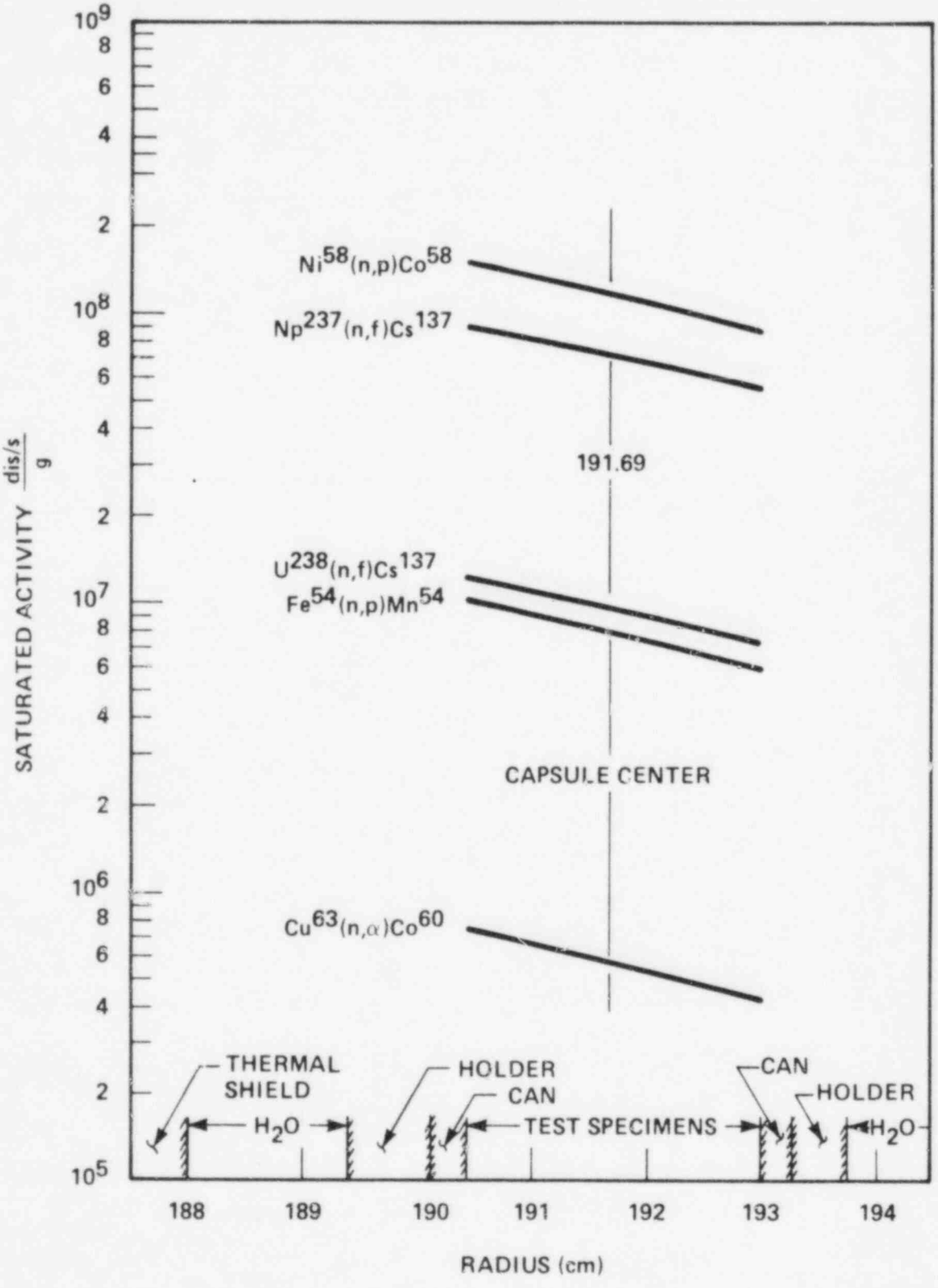

Figure 6-7. Calculated Variation of Fast Neutron Flux Monitor Saturated Activity Within Capsule T

TABLE 6-3

CALCULATED FAST NEUTRON FLUX (E > 1.0 MeV) AND LEAD FACTORS FOR H. B. ROBINSON UNIT 2 SURVEILLANCE CAPSULES

Azimuthal Location (deg)	Φ(E > 1.0 MeV) (n/cm^2-sec)	Lead Factor
0	1.68×10^{11}	2.63
10	1.20×10^{11}	1.88
20	4.85×10^{10}	0.76
30	3.71×10^{10}	0.58
40	2.31×10^{10}	0.36

TABLE 6-4

CALCULATED NEUTRON ENERGY SPECTRA AT THE CENTER OF THE H. B. ROBINSON UNIT 2 SURVEILLANCE CAPSULES

Group No.	Neutron Flux (n/cm^2-sec)				
	0 deg	10 deg	20 deg	30 deg	40 deg
1	1.24×10^{9}	8.66×10^{8}	5.04×10^{8}	3.73×10^{8}	2.73×10^{8}
2	4.12×10^{9}	2.89×10^{9}	1.71×10^{9}	1.27×10^{9}	9.41×10^{8}
3	6.79×10^{9}	4.71×10^{9}	2.49×10^{9}	1.86×10^{9}	1.30×10^{9}
4	7.54×10^{9}	5.23×10^{9}	2.45×10^{9}	1.85×10^{9}	1.22×10^{9}
5	1.20×10^{10}	8.32×10^{9}	3.56×10^{9}	2.72×10^{9}	1.73×10^{9}
6	2.32×10^{10}	1.62×10^{10}	6.77×10^{9}	5.19×10^{9}	3.23×10^{9}
7	3.02×10^{10}	2.15×10^{10}	8.51×10^{9}	6.54×10^{9}	4.01×10^{9}
8	3.92×10^{10}	2.83×10^{10}	1.08×10^{10}	8.26×10^{9}	4.99×10^{9}
9	4.38×10^{10}	3.21×10^{10}	1.17×10^{10}	8.98×10^{9}	5.42×10^{9}
10	4.37×10^{10}	3.21×10^{10}	1.16×10^{10}	8.89×10^{9}	5.33×10^{9}
11	1.36×10^{11}	1.01×10^{11}	3.51×10^{10}	2.68×10^{10}	1.60×10^{10}
12	1.64×10^{11}	1.23×10^{11}	4.14×10^{10}	3.16×10^{10}	1.86×10^{10}
13	7.86×10^{10}	5.86×10^{10}	1.96×10^{10}	1.50×10^{10}	8.72×10^{9}
14	6.36×10^{10}	4.74×10^{10}	1.57×10^{10}	1.21×10^{10}	7.03×10^{9}
15	5.22×10^{10}	3.87×10^{10}	1.29×10^{10}	9.92×10^{9}	5.75×10^{9}
16	1.21×10^{11}	9.00×10^{10}	2.96×10^{10}	2.27×10^{10}	1.32×10^{10}
17	1.03×10^{11}	7.64×10^{10}	2.49×10^{10}	1.91×10^{10}	1.11×10^{10}
18	1.06×10^{11}	7.95×10^{10}	2.56×10^{10}	1.97×10^{10}	1.13×10^{10}
19	8.80×10^{10}	6.51×10^{10}	2.10×10^{10}	1.62×10^{10}	9.24×10^{9}
20	1.01×10^{11}	7.40×10^{10}	2.41×10^{10}	1.85×10^{10}	1.06×10^{10}
21	2.75×10^{11}	1.77×10^{11}	6.72×10^{10}	5.09×10^{10}	2.93×10^{10}

TABLE 6-5

SPECTRUM AVERAGED REACTION CROSS SECTIONS AT THE DOSIMETER BLOCK LOCATION FOR H. B. ROBINSON UNIT 2 SURVEILLANCE CAPSULES

Reaction	$\bar{\sigma}$ (barns)				
	0 deg	10 deg	20 deg	30 deg	40 deg
$Fe^{54}(n,p)\ Mn^{54}$	0.749	.0729	.0900	.0882	.0970
$Ni^{58}(n,p)\ Co^{58}$	.100	.0979	.117	.115	.125
$Cu^{63}(n,\alpha)Co^{60}$	.000533	.000522	.000753	.000730	.000861
$U^{238}(n,f)$ F.P.	.365	.362	.382	.380	.389
$Np^{237}(n,f)$ F.P.	2.57	2.61	2.47	2.47	2.45

reactor pressure vessel is shown. The relative axial variation of neutron flux within the vessel is given in figure 6-5. Absolute axial variations of fast neutron flux may be obtained by multiplying the levels given in figure 6-3 or 6-4 by the appropriate values from figure 6-5.

In figure 6-6 the radial variations of fast neutron flux within surveillance Capsule T are presented. These data, in conjunction with the maximum vessel flux, are used to develop lead factors for each of the capsules. Here the lead factor is defined as the ratio of the fast neutron flux ($E > 1.0$ MeV) at the dosimeter block location (capsule center) to the maximum fast neutron flux at the pressure vessel inner radius. Updated lead factors for all of the H. B. Robinson Unit 2 surveillance capsules are listed in table 6-3.

Since the neutron flux monitors contained within the surveillance capsules are not all located at the same radial location, the measured disintegration rates are analytically adjusted for the gradients that exist within the capsules so that flux and fluence levels may be derived on a common basis at a common location. This point of comparison was chosen to be the capsule center. Analytically determined reaction rate gradients for use in the adjustment procedures are shown in figure 6-7 for Capsule T. All of the applicable fast neutron reactions are included.

In order to derive neutron flux and fluence levels from the measured disintegration rates, suitable spectrum-averaged reaction cross sections are required. The neutron energy spectrum calculated to exist at the center of each of the H. B. Robinson Unit 2 surveillance capsules is given in table 6-4. The associated spectrum-averaged cross sections for each of the five fast neutron reactions are given in table 6-5.

6-5. DOSIMETRY RESULTS

The irradiation history of the H. B. Robinson Unit 2 reactor is given in table 6-6. Comparisons of measured and calculated saturated activity of the flux monitors contained in Capsule T are listed in

TABLE 6-6

IRRADIATION HISTORY OF CAPSULE T

Month	Year	Pj(MW)	P_{max}(MW)	P_j/P_{max}	Irradiation Time (Days)	Decay Time (Days)
7	1971	1541	2300	.670	31	4089
8	1971	1541	2300	.670	31	4058
9	1971	1593	2300	.692	30	4028
10	1971	1541	2300	.670	31	3997
11	1971	1903	2300	.827	30	3967
12	1971	2207	2300	.960	31	3936
1	1972	2044	2300	.889	31	3905
2	1972	2241	2300	.974	29	3876
3	1972	2235	2300	.972	31	3845
4	1972	2208	2300	.960	30	3815
5	1972	402	2300	.175	31	3784
6	1972	1357	2300	.590	30	3754
7	1972	1626	2300	.707	31	3723
8	1972	1967	2300	.855	31	3692
9	1972	2031	2300	.883	30	3662
10	1972	2099	2300	.912	31	3631
11	1972	902	2300	.827	30	3601
12	1972	1498	2300	.651	31	3570
1	1973	1216	2300	.529	31	3539
2	1973	1196	2300	.520	28	3511
3	1973	819	2300	.356	31	3480
4	1973	0	2300	.000	30	3450
5	1973	436	2300	.189	31	3419
6	1973	1821	2300	.792	30	3389
7	1973	1847	2300	.803	31	3358
8	1973	2006	2300	.872	31	3327
9	1973	2063	2300	.897	30	3297
10	1973	2031	2300	.883	31	3266
11	1973	1583	2300	.688	30	3236
12	1973	1952	2300	.849	31	3205
1	1974	2082	2300	.905	31	3174
2	1974	2162	2300	.940	28	3146
3	1974	2226	2300	.968	31	3115
4	1974	2179	2300	.947	30	3085
5	1974	315	2300	.137	31	3054

TABLE 6-6 (cont)
IRRADIATION HISTORY OF CAPSULE T

Month	Year	Pj(MW)	P_{max}(MW)	Pj/P_{max}	Irradiation Time (Days)	Decay Time (Days)
6	1974	161	2300	.070	30	3024
7	1974	2028	2300	.882	31	2993
8	1974	1949	2300	.848	31	2962
9	1974	1994	2300	.867	30	2932
10	1974	1991	2300	.865	31	2901
11	1974	2239	2300	.973	30	2871
12	1974	2280	2300	.991	31	2840
1	1975	2090	2300	.909	31	2809
2	1975	2255	2300	.980	28	2761
3	1975	2167	2300	.942	31	2750
4	1975	795	2300	.346	30	2720
5	1975	298	2300	.130	31	2689
6	1975	1738	2300	.756	30	2659
7	1975	1976	2300	.859	31	2628
8	1975	2130	2300	.926	31	2597
9	1975	2051	2300	.892	30	2567
10	1975	2125	2300	.924	31	2536
11	1975	0	2300	.000	30	2506
12	1975	1133	2300	.493	31	2475
1	1976	1899	2300	.826	31	2444
2	1976	2267	2300	.986	29	2415
3	1976	2194	2300	.954	31	2384
4	1976	2132	2300	.927	30	2354
5	1976	1925	2300	.837	31	2323
6	1976	2166	2300	.943	30	2293
7	1976	1988	2300	.864	31	2262
8	1976	2066	2300	.898	31	2231
9	1976	2133	2300	.927	30	2201
10	1976	1991	2300	.866	31	2170
11	1976	0	2300	.000	30	2140
12	1976	1044	2300	.454	31	2109
1	1977	2181	2300	.948	31	2078
2	1977	1170	2300	.509	28	2050
3	1977	1987	2300	.864	31	2019
4	1977	1726	2300	.750	30	1989

TABLE 6-6 (cont)
IRRADIATION HISTORY OF CAPSULE T

Month	Year	Pj(MW)	P_{max}(MW)	Pj/P_{max}	Irradiation Time (Days)	Decay Time (Days)
5	1977	2138	2300	.930	31	1958
6	1977	2036	2300	.885	30	1928
7	1977	1890	2300	.822	31	1897
8	1977	1502	2300	.653	31	1866
9	1977	940	2300	.409	30	1836
10	1977	1047	2300	.455	31	1805
11	1977	275	2300	.120	30	1775
12	1977	2126	2300	.924	31	1744
1	1978	1778	2300	.773	31	1713
2	1978	0	2300	.000	28	1685
3	1978	0	2300	.000	31	1654
4	1978	200	2300	.087	30	1624
5	1978	2036	2300	.885	31	1593
6	1978	2106	2300	.916	30	1563
7	1978	1643	2300	.715	31	1532
8	1978	2067	2300	.899	31	1501
9	1978	1477	2300	.642	30	1471
10	1978	2176	2300	.947	31	1440
11	1978	2193	2300	.953	30	1410
12	1978	2120	2300	.922	31	1379
1	1979	2055	2300	.893	31	1348
2	1979	2007	2300	.872	28	1320
3	1979	2180	2300	.948	31	1289
4	1979	678	2300	.295	30	1259
5	1979	0	2300	.000	31	1226
6	1979	0	2300	.000	30	1198
7	1979	475	2300	.207	31	1167
8	1979	2162	2300	.940	31	1136
9	1979	2050	2300	.891	30	1106
10	1979	2104	2300	.915	31	1075
11	1979	2147	2300	.933	30	1045
12	1979	2157	2300	.938	31	1014
1	1980	2204	2300	.958	31	983
2	1980	2163	2300	.940	29	954
3	1980	1192	2300	.518	31	923

TABLE 6-6 (cont)
IRRADIATION HISTORY OF CAPSULE T

Month	Year	Pj(MW)	P_{max}(MW)	Pj/P_{max}	Irradiation Time (Days)	Decay Time (Days)
4	1980	899	2300	.391	30	893
5	1980	1367	2300	.594	31	862
6	1980	1994	2300	.867	30	832
7	1980	1093	2300	.475	31	801
8	1980	219	2300	.095	31	770
9	1980	0	2300	.000	30	740
10	1980	228	2300	.099	31	709
11	1980	1912	2300	.831	30	679
12	1980	401	2300	.174	31	648
1	1981	1595	2300	.693	31	617
2	1981	1930	2300	.839	28	589
3	1981	2196	2300	.955	31	558
4	1981	2141	2300	.931	30	528
5	1981	989	2300	.430	31	497
6	1981	1108	2300	.482	30	467
7	1981	1817	2300	.790	31	436
8	1981	0	2300	.000	31	405
9	1981	922	2300	.401	30	375
10	1981	1058	2300	.460	31	344
11	1981	239	2300	.104	30	314
12	1981	1391	2300	.605	31	283
1	1982	1825	2300	.793	31	252
2	1982	1677	2300	.729	28	224

table 6-7. The data are presented as measured at the actual monitor locations as well as adjusted to the capsule center. All adjustments to the capsule center were based on the data presented in figure 6-7.

The fast neutron ($E > 1.0$ MeV) flux and fluence levels derived for Capsule T are presented in table 6-8. The thermal neutron flux obtained from the cobalt-aluminum monitors is summarized in table 6-9. Due to the relatively low thermal neutron flux at the capsule locations, no burnup correction was made to any of the measured activities. The maximum error introduced by this assumption is estimated to be less than 1 percent for the Ni^{58} (n,p) Co^{58} reaction and even less significant for all of the other fast neutron reactions.

TABLE 6-7

COMPARISON OF MEASURED AND CALCULATED FAST NEUTRON FLUX MONITOR SATURATED ACTIVITIES FOR CAPSULE T

Reaction and Axial Location	Radial Location (cm)	Saturated Activity dis/s / g		Adjusted Saturated Activity dis/s / g	
		Capsule T	Calculated	Capsule V	Calculated
$Fe^{54}(n,p)Mn^{54}$					
R-63	191.47	9.05×10^6	8.35×10^6	8.62×10^6	
H-17	191.47	8.93×10^6	8.35×10^6	8.51×10^6	
R-57	191.47	9.78×10^6	8.35×10^6	9.32×10^6	
W-18	192.47	7.53×10^6	6.65×10^6	9.01×10^6	
L-42	192.47	7.47×10^6	6.65×10^6	8.94×10^6	
L-48	192.47	7.38×10^6	6.65×10^6	8.83×10^6	
Average				8.87×10^6	7.96×10^6
$Cu^{63}(n,\alpha)Co^{60}$					
Top	191.47	7.90×10^5	5.98×10^5	7.53×10^5	
Bottom	191.47	8.26×10^5	5.98×10^5	7.87×10^5	
Average				7.70×10^5	5.70×10^5
$Ni^{58}(n,p)Co^{58}$					
Middle	191.47	1.31×10^8	1.22×10^8	1.24×10^8	1.16×10^8
$Np^{237}(n,f)Cs^{137}$					
Middle	191.70	8.72×10^7	7.15×10^7	8.72×10^7	7.15×10^7
$U^{238}(n,f)Cs^{137}$[a]					
Middle	191.70	1.32×10^7	9.65×10^6	1.32×10^7	9.65×10^6

a Includes a 20 percent correction for U^{235} fissions and Pu^{239} production

Using the iron data presented in table 6-8, along with the lead factors given in table 6-3, the fast neutron fluence ($E > 1.0$ MeV) for Capsule T as well as for the reactor vessel inner diameter is summarized in table 6-10. The agreement between calculation and measurement is excellent with a measured fluence level of 4.11×10^{19} n/cm^2 compared to a calculated value of 3.81×10^{19} n/cm^2 for Capsule T.

TABLE 6-8

RESULTS OF FAST NEUTRON DOSIMETRY FOR CAPSULE T

Reaction	Adjusted Saturated Activity $\frac{dis/s}{g}$		ϕ (E > 1.0 MeV) (n/cm^2-sec)		Φ (E > 1.0 MeV) (n/cm^2)	
	Measured	Calculated	Measured	Calculated	Measured	Calculated
$Fe^{54}(n,p)Mn^{54}$	8.87×10^6	7.96×10^6	1.81×10^{11}	1.68×10^{11}	4.11×10^{19}	3.81×10^{19}
$Cu^{63}(n,\alpha)Co^{60}$	7.70×10^5	5.70×10^5		2.19×10^{11}		4.97×10^{19}
$Ni^{58}(n,p)Co^{58}$	1.24×10^8	1.16×10^8		1.77×10^{11}		4.02×10^{19}
$Np^{237}(n,f)Cs^{137}$	8.72×10^7	7.15×10^7		2.05×10^{11}		4.65×10^{19}
$U^{238}(n,f)Cs^{137}$	1.32×10^7	9.65×10^6		2.27×10^{11}		5.16×10^{19}

Note: Irradiation time equals 2.27×10^8 EFPS

TABLE 6-9

RESULTS OF THERMAL NEUTRON DOSIMETRY FOR CAPSULE T

Axial Location	Saturated Activity $\frac{dis/s}{g}$		ϕ_{Th} (n/cm^2-sec)
	Bare	Cd-Covered	
Top	1.24×10^8	5.62×10^7	1.20×10^{11}
Middle	Not Measured	6.04×10^7	1.34×10^{11}[a]
Bottom	1.48×10^8	6.11×10^7	1.55×10^{11}

a. Thermal neutron flux at the middle position is based on a bare wire activity equal to the average of the top and bottom measurements.

Also listed in table 6-10 is a comparison of calculated values with the average value of all dosimeter measurements. Again, the agreement is good and within the assigned uncertainty of plus or minus 20 percent for the analytical predictions.

TABLE 6-10

SUMMARY OF NEUTRON DOSIMETRY RESULTS FOR CAPSULE T

Basis	Irradiation Time (EFPS)	ϕ (E > 1.0 MeV) (n/cm^2-sec)	Φ (E > 1.0 MeV) (n/cm^2)	Lead Factor	Vessel Fluence (n/cm^2)	Vessel Fluence (calculated) (n/cm^2)
$Fe^{54}(n,p)Mn^{54}$	2.27 ~~2.17~~ x 10^8	1.81 x 10^{11}	4.11 x 10^{19}	2.63	1.56 x 10^{19}	1.45 x 10^{19}
Dosimeter Avg	2.27 x 10^8	2.02 x 10^{11}	4.58 x 10^{19}	2.83	1.74 x 10^{19}	1.45 x 10^{19}

REFERENCES

1. Yanichko, S. E., "Carolina Power And Light Co., H. B. Robinson Unit No. 2 Reactor Vessel Radiation Surveillance Program," WCAP-7373, January, 1970.

2. Yanichko, S. E., et al, "Analysis of Capsule S From Carolina Power and Light Co., H. B. Robinson Unit 2 Reactor Vessel Radiation Surveillance Program," WCAP-8249, December 18, 1973.

3. Norris, E. B. "Reactor Vessel Material Surveillance Program For H. B. Robinson Unit 2 Analysis of Capsule V," Final Report - SWRI Project No. 02-4397, October 19, 1976.

4. Letter From E. B. Norris, Southwest Research Institute To Talmadge Clements, Carolina Power and Light Co., "H. B. Robinson Unit 2 Reactor Vessel Material Surveillance Program," April 4, 1977

5. Soltesz, R. G., et al., *Final Progress Report, Nuclear Rocket Shielding Methods, Modification, Updating, and Input Data Preparation, Vol. 5, Two-Dimensional Discrete Ordinates Transport Technique,* WANL-PR(LL)034, August, 1970.

6. Collier, G., et al, *Second Version of the GAMB1T Code,* WANL-TME-1969, November 1969.

7. Soltesz, R. G., et al, *Final Progress Report, Nuclear Rocket Shielding Methods, Modification, Updating, and Input Data Preparation, Vol. 3, Cross Section Generation and Data Processing Techniques,* WANL-PR(LL)034, August 1970.

8. Soltesz, R. G., et al, *Final Progress Report, Nuclear Rocket Shielding Methods, Modification, Updating, and Input Data Preparation, Vol. 4, One-Dimensional Discrete Ordinates Transport Technique,* WANL-PR(LL)034, August 1970.

9. ASTM E 261-77, "Standard Practice for Measuring Neutron Flux, Fluence, and Spectra by Radioactivation Techniques." *1981 Annual Book of ASTM Standards.* Part 45 Nuclear Standards pp 915-926 Philadelphia: American Society for Testing and Materials, 1981

10. ASTM E 262-77, "Standard Test Method for Measuring Thermal Neutron Flux by Radioactivation Techniques." *1981 Annual Book of ASTM Standards.* Part 45 Nuclear Standards. pp 927-935 Philadelphia: American Society for Testing and Materials, 1981.

11. ASTM E 263-77, "Standard Test Method for Measuring Fast-Neutron Flux by Radioactivation of Iron," *1981 Annual Book of ASTM Standards.* Part 45 Nuclear Standards. pp 936-941 Philadelphia: American Society for Testing and Materials, 1981.

12. ASTM E 481-78, "Standard Method for Measuring Neutron-Flux Density by Radioactivation of Cobalt and Silver," *1981 Annual Book of ASTM Standards.* Part 45 Nuclear Standards. pp 1063-1070 Philadelphia: American Society for Testing and Materials, 1981.

13. ASTM E 264-77, "Standard Test Method for Measuring Fast-Neutron Flux by Radioactivation of Nickel." *1981 Annual Book of ASTM Standards.* Part 45 Nuclear Standards. pp 942-945 Philadelphia: American Society for Testing and Materials, 1981.